Review

Non-aqueous rechargeable aluminum-ion batteries (RABs): recent progress and future perspectives

Sahithi Thatipamula[1], Chamali Malaarachchi[1], Md Robiul Alam[1], Muhammad Waqas Khan[1], Ravichandar Babarao[2,3], Nasir Mahmood[1] (ORCID)

[1]School of Sciences, RMIT University, Melbourne 3000, Australia.
[2]School of Science, Centre for Advanced Materials and Industrial Chemistry (CAMIC), RMIT University, Melbourne 3001, Australia.
[3]ARC Centre of Excellence for Green Electrochemical Transformation of Carbon Dioxide, School of Science, RMIT University, Melbourne 3000, Australia.

Correspondence to: Dr. Muhammad Waqas Khan, School of Sciences, RMIT University, 124 La Trobe Street, Melbourne 3000, Australia. E-mail: muhammad.waqas.khan@rmit.edu.au; Dr. Nasir Mahmood, School of Sciences, RMIT University, 124 La Trobe Street, Melbourne 3000, Australia. E-mail: nasir.mahmood@rmit.edu.au

Abstract

To meet the growing energy demand, it is imperative to explore novel materials for batteries and electrochemical chemistry beyond traditional lithium-ion batteries. These innovative batteries aim to achieve long cycle life, capacity, and enhanced energy densities. Rechargeable aluminum batteries (RABs) have gained attention due to their high safety, cost-effectiveness, straightforward manufacturing process, environmental friendliness, and extended lifespan. Despite aluminum having advantages as the anode in achieving high energy density, RAB technology is yet in its early stages, necessitating substantial efforts to overcome fundamental and practical challenges. This comprehensive review centers on the historical development of aluminum batteries, delve into the electrode development in non-aqueous RABs, and explore advancements in non-aqueous RAB technology. It also encompasses essential characterizations and simulation techniques crucial for understanding the underlying mechanisms. By addressing challenges in battery components, this review proposes feasible strategies to improve the electrochemical performance and safety of RABs and the development of hybrid lithium/aluminum batteries. In conclusion, it provides perspectives on endeavors in this field that aim to bridge the gap between laboratory research and real-world applications of RABs.

Keywords: Rechargeable aluminum batteries, aluminum alloys, hybrid Li-Al, non-aqueous electrolyte, challenges, energy storage.

INTRODUCTION

Recently, the increasing emission of greenhouse gases and continued dependence on fossil energy sources have raised widespread concerns, highlighting the urgent need to explore and harness new energy alternatives[1]. This has led to a heightened focus on renewable energy sources such as solar energy and wind. However, the effective utilization of these sources often requires support from high-efficiency energy storage devices, given their uneven distribution in both time and space[2]. The roots of lithium-ion batteries (LIBs) started back in the 1970s when the metal lithium was used as an anode. Notably, research since the 1980s delved into Li_xMO_2 (M = Mn, V, Co, Ni) as a cathode for LIBs, resulting in Sony Corporation producing the first commercial LIB in 1991[3,4]. LIBs have since experienced remarkable development with applications in widespread domains, including grid-scale energy storage, electric automobiles, and portable electronic devices. Despite their successes, LIBs face challenges such as safety concerns, short cycling life, and limited availability of lithium resources, hindering their further progress[5,6].

The aqueous rechargeable aluminum battery (RAB) systems are generally convenient in handling, cost-effective, and offer relatively high conductivity, low viscosity, and low flammability. However, they have not succeeded in incorporating aluminum into the commercial-level batteries as the formation of a passivating oxide layer has been causing the actual cell voltage to be significantly lower than its theoretical value. Additionally, a delayed action occurs, resulting in a time lag before the cell reaches its maximum voltage when the circuit is closed. This delay is attributed to the gradual removal of the oxide layer from the aluminum anode surface. Even though the oxide layer can be dissolved with acidic, alkaline, or saline media, it can prompt a corrosive environment for the elements in the battery. Further, parasitic hydrogen generation has also been attributed to wasteful corrosion, making it less efficient and durable.

To address the growing demands for energy-driven applications, the need for new high-performance battery systems has become imperative[7,8]. A sustainable development strategy requires the creation of a competitive chemical power system that is cost-effective, safe, durable, and possesses high energy density, utilizing more abundantly available metals. Among the non-lithium alternatives, batteries based on Mg, Na, Mn, Al, K, Zn, and Ca have been identified as promising candidates[9,10].

Figure 1 provides a detailed comparison of various metal anodes, considering factors such as gravimetric capacity, standard potential, availability in the earth's crust, and volumetric capacity[11,12]. While batteries utilizing aluminum as an anode showcase promise due to their low cost and high performance, there are still certain limitations to consider. One significant constraint lies in the early stages of development of RABs[13,14]. Overcoming fundamental and practical challenges is an ongoing process, and substantial efforts are required to optimize their electrochemical performance and safety. Additionally, the technology is not yet widely adopted, and there may be hurdles in scaling up production to meet larger energy storage demands. The motivation behind exploring batteries with aluminum as an anode is compelling[15,16]. The cost-effectiveness and high performance of these batteries make them an attractive alternative for various applications. Aluminum having higher electronegativity, ensuring lower reactivity, is crucial to enhanced safety, especially in humid conditions[17]. As the world seeks sustainable and efficient energy solutions, the development of RABs aligns with the imperative to create competitive chemical power systems that are economically viable, safe, durable, and possess high energy density[18,19]. The potential of RABs to address these criteria provides strong motivation for further research and development in this field.
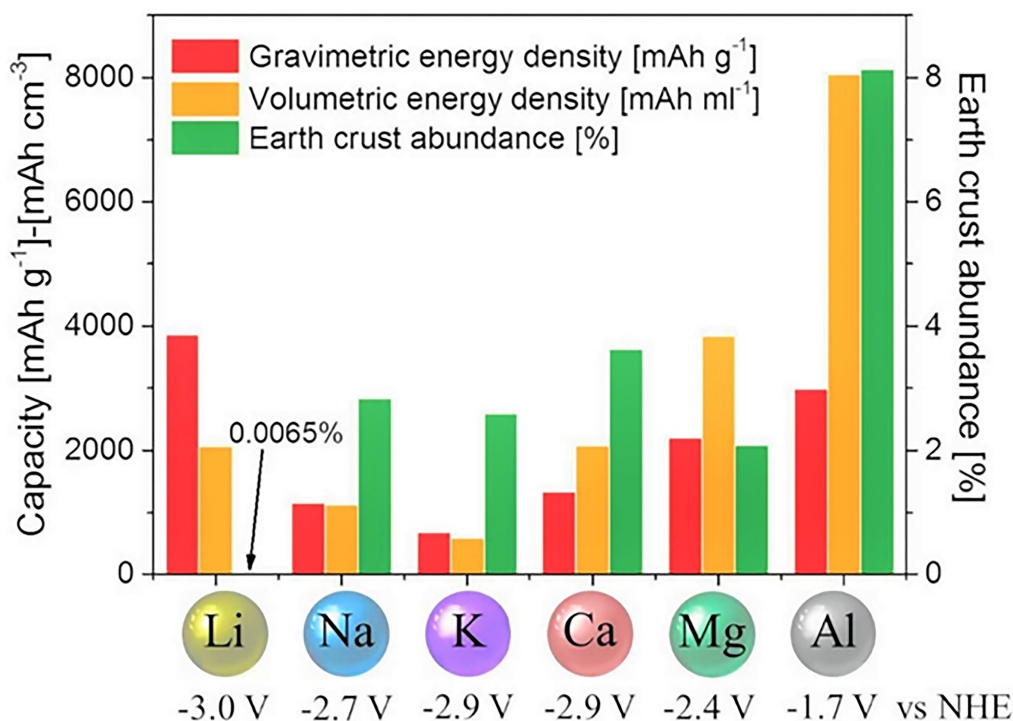
Figure 1. Comparison of gravimetric and volumetric energy density and earth crust abundance. Reproduced with permission ref.[6] Copyright 2016 Wiley.

To deeply understand how aluminum batteries work, let us examine Figure 2 to see how they have evolved. Aluminum batteries are of two types: primary and secondary. Aluminum was first used as an anode for the Al/HNO$_3$/C cell back in 1857[7]. In 1948, a heavy-duty Al-Cl$_2$ battery was developed, featuring amalgamated aluminum as an anode[20]. In 1962, in a primary aluminum-air battery (AAB) using a concentrated KOH or NaOH solution, researchers showcased the reversible aluminum stripping/plating behaviors in molten salt electrolytes[21,22]. This demonstration laid the foundational groundwork for assembling rechargeable battery systems. In 1988, an initial investigation was conducted into a secondary battery using Al/AlCl$_3$/NaCl/FeS$_2$ at temperatures ranging from 180 to 300 °C. This exploration revealed enhanced capacity and discharge plateau, aided by CoS, graphite, and CuS. A room-temperature ionic liquid (RTIL) electrolyte, composed of AlCl$_3$ and 1,2-Dimethyl-3-propyl imidazolium chloride (DMPrlCl) at a molar ratio of 1:1.5, was employed for an Al-graphite battery with an average discharge voltage of 1.7 V and exhibited a discharge capacity of up to 35-40 mAhg^{-1} and sustaining over 150 cycles. Nevertheless, the battery's reaction mechanism shares similarities with the Al-Cl$_2$ battery[23]. In the 1980s, companies started opting for lithium batteries for their high capacity and voltage, which is an added advantage. Nonetheless, the advancement of RABs has been significantly hindered by their low discharge voltage, lifespan, and low energy density. However, lithium batteries have significant disadvantages in terms of safety and limited lithium resources in the earth's crust; therefore, research on aluminum battery development has been reignited. In 2010, the idea of a secondary aluminum battery utilizing spinel λ-Mn$_2$O$_4$ as a viable cathode material within an RTIL of AlCl$_3$/1-ethyl-3methyimidazolium chloride (EMIC) was explored. Unfortunately, the initial tests yielded no intercalation capacity[24]. Then, a novel aluminum battery variant employing graphite, which is used as a cathode, was introduced in 2015, delivering high voltage, cost-effectiveness, and safety[25]. In 2016, a groundbreaking hybrid, Al-Li batteries, was created, using aluminum as an anode and LiFePO$_4$ as the cathode. This battery operated within an AlCl$_3$/EMIC ionic liquid (IL) with LiAlCl$_4$. The expected reversibility of the electrochemical redox reactions occurred due to the stripping/deposition of aluminum at the aluminum
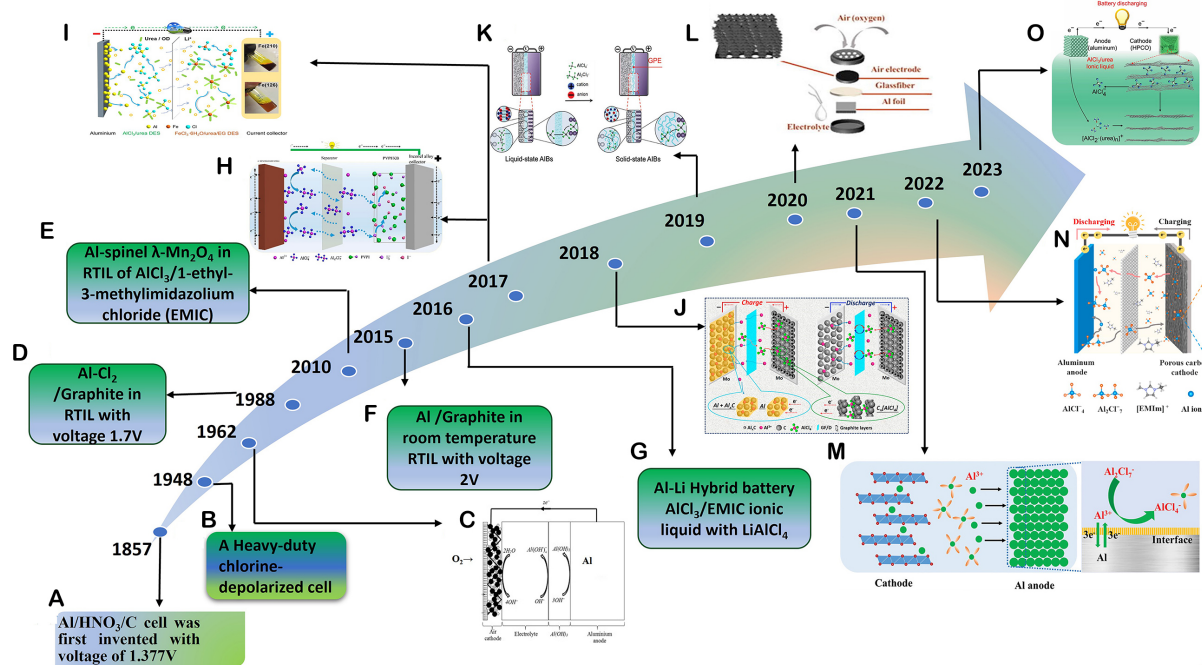
Figure 2. An overview of the development of Al-based batteries. (A) Aluminum served as an anode in the buff cell[7]. (B) A heavy-duty chlorine depolarized cell[20]. (C) Aluminum-air primary battery. Reproduced with permission ref.[22] copyright 2013 Elsevier. (D) Proposed Al-Cl$_2$ with graphite cathode[23]. (E) The Secondary cell based on room temperature ionic liquid[24]. (F) Invention of Aluminum-Graphite with room temperature ionic liquid[25]. (G) Hybrid Aluminum-Lithium battery with lithium as an anode[26]. (H) Rechargeable Al-I$_2$ battery schematic. Reproduced with permission ref.[28] copyright 2017 American Chemical Society. (I) The Aluminum-Iron hybrid liquid battery. Reproduced with permission ref.[27] copyright 2017 Elsevier. (J) The battery featuring dual graphite electrodes. Reproduced with permission ref.[29] copyright 2018 Elsevier. (K) The solid-state Aluminum-graphite battery with gel-polymer electrolyte. Reproduced with permission ref.[30] copyright 2018 Wiley-VCH. (L) Ultrathin Co$_3$O$_4$ nanosheets as binder-free cathodes for aluminum-air batteries. Reproduced with permission ref.[31] copyright 2020 Elsevier. (M) Anode and electrolyte interface for non-aqueous aluminum-ion batteries. Reproduced with permission ref.[11] copyright 2021 Wiley-VCH. (N) Alcl$_4^-$ ion storage by activated carbon in non-aqueous aluminum-ion battery. Reproduced with permission ref.[32] copyright 2022 Elsevier. (O) Aluminum/pours carbon graphite with urea as electrolyte. Reproduced with permission ref.[33] copyright 2023 Elsevier.

electrode, and the Li intercalation/deintercalation occurred at the LiFePO$_4$ electrode throughout the charge-discharge process[26]. In 2017, an aluminum-graphite battery system with a molten-salt rechargeable operating within an acidic AlCl$_3$/NaCl electrolyte at temperatures exceeding 120 °C. Furthermore, an aluminum-graphite battery was engineered utilizing an IL analog electrolyte comprising AlCl$_3$ and urea. This electrolyte system is highlighted for being environmentally friendly and low-cost. Al-I$_2$ batteries featuring the I$_3$-I-redox chemistry employed a polyvinylpyrrolidone-I$_2$ complex to use as the cathode along with the AlCl$_3$/EMIC IL. A cost-effective and high-energy Al-Fe hybrid liquid battery was developed using an iron-based deep eutectic solvent and an aluminum-based solvent[27]. Considering the corrosion problem associated with aluminum anodes, a novel aluminum battery was introduced in 2018, employing a dual-graphite configuration[28,29]. In 2019, to overcome the issues encountered by the mechanical deformation interface and gases from the glass fiber separator with insufficient electrolyte problems to overcome it, a solid-state gel polymer electrolyte (GPE) was used for the aluminum-graphite battery[30]. Among the next advancements, binder-free cathodes have secured a prominent place, and for instance, the cathode material with ultrathin Co$_3$O$_4$ nanosheets that are anchored onto N-doped carbon nanotubes (CNTs) and then grafted onto a 3D graphene structure by a nickel substrate can be considered, where it has enabled achieving a capacity of 483.30 mAhg^{-1}. This battery showcased remarkable cycling longevity, enduring over 600 cycles while maintaining a consistent discharge capacity of around 70 mAhg^{-1} at 20 mAg^{-1}[31]. The aluminum anode and IL electrolyte pose challenges due to the corrosive nature of aluminum. Efforts have been initiated to

design the interface between the anode and the electrolyte in non-aqueous aluminum batteries, particularly focusing on exploring surface modifications[11]. The creation of low-cost, highly defective mesoporous-activated carbon from coconut shells, followed by activation with KOH, has resulted in a cathode material for RABs. This material exhibited a discharge capacity of 150 mAhg^{-1} at 0.1 A and maintained stability even after 1,500 cycles[32]. The hierarchical porous carbon octahedron (HCPO) was synthesized from the copper-based metal-organic framework (MOF), while aluminum was used as anode in an AlCl$_3$/Urea IL electrolyte with a specific capacity of 60.8 mAhg^{-1} after 200 cycles at 100 mAg^{-1}[33].

This comprehensive review article aims to provide a thorough overview of the latest progress in aluminum batteries. The historical perspectives assess the progress made in non-aqueous RABs and the current advancements in aluminum batteries that contribute to a deeper understanding of electrochemical processes and technology. This review focuses on pinpointing major challenges and addressing essential issues. Additionally, this review will provide feasible strategies to guide the continued development of aluminum batteries to attain practical energy storage requirements of various applications.

DEVELOPMENT OF ALUMINUM-ION BATTERIES

Al, securing the third place among the most abundant elements on Earth, has been identified as a good candidate for the anode in metal-ion batteries due to its trivalent nature and, therefore, having a high theoretical volumetric capacity (8,040 mAhcm^{-3}), which is nearly four times than that of Li (2,040 mAhcm^{-3})[34]. Further, it has a gravimetric capacity comparable to Li, with values of 3.0 Ahg^{-1} and 3.8 Ahg^{-1}[35], respectively, for Al and Li. Therefore, tremendous attention has been drawn to the development of aluminum batteries within the last few years, and numerous research studies are ongoing. Like other types of batteries, aluminum batteries are classified into two categories, primary and secondary, based on their recharging capability. The initial developments typically have fallen into the primary section due to their inability to recharge, while efforts to develop secondary aluminum batteries were initiated in 1980[20-22,36].

Primary batteries

Primary batteries basically use aqueous electrolytes, where alkalinity has been the most preferred in relevant studies. These batteries must be discarded upon discharging due to the non-reversibility of the redox reactions. Initial studies in the context of aluminum batteries generally fall into this category, and it includes the battery developed in 1855 by M. Hulot in which Al has been used as the cathode rather than the anode, along with an amalgamate of Zn and Hg as the cathode and dilute sulfuric acid as the electrolyte[37,38]. Then, with further evolvement, Al marked its first use as the anode in 1857. This battery has been known as a Buff battery, and the aluminum anode is combined with a carbon cathode. Followed by different concepts, including the use of an amalgamated Al-Zn alloy anode with a carbon cathode, the first Leclanché type dry cell was developed in the 1950s using an aluminum anode and a MnO$_2$ cathode along with NaOH and ZnO as the electrolyte[7].

The use of aqueous systems is generally convenient and inexpensive for handling, and it has comparatively high conductivity of ions, low viscosity, and low flammability. However, these have not succeeded in taking Al into the commercial-level batteries, as the formation of a passivating oxide layer causes the actual cell voltage to be significantly lower than its theoretical value. In addition, a delayed action resulted in a time lag till the cell operates at the maximum voltage when the circuit is closed. This delay is ascribed to the gradual depletion of the oxide layer from the aluminum anode surface. Even though the oxide layer can be dissolved with acidic, alkaline, or saline media, it can create a corrosive environment for the elements in the battery. Furthermore, parasitic hydrogen generation has also been attributed to wasteful corrosion, making it less efficient and durable.

Secondary batteries

Secondary batteries are rechargeable batteries where the redox reactions can be restored to the original condition by regenerating the original chemical reactants with a current provided in the opposite direction to the current while discharging. Due to their rechargeability, these batteries have a longer shelf life, making them more cost-effective and environmentally friendlier than primary batteries. The inclusion of aqueous electrolytes in secondary aluminum batteries has been reported to be not feasible as the electrode potential of Al^{3+}/Al is more negative than that of H^+/H_2, and hence, electrochemical reversible plating/stripping is not possible as hydrogen evolution is more prominent rather than Al deposition[39]. Therefore, molten salts or non-aqueous media have always been the choice for secondary aluminum batteries. Even though initial studies have been based on molten salt electrolytes, chloroaluminate-based ILs have been frequently utilized due to the complexity provoked by high operating temperatures. Imidazole-based organic chlorides, including 1-ethyl-3-methylimidazolium chloride[40,41] (EMIC) or 1-butyl-3-methylimidazolium chloride[27] (BMIC) with $AlCl_3$, have been the players in this context despite their drawbacks related to corrosiveness, expensiveness, hygroscopic nature, and leading to unwanted reactions such as $AlCl_4^-$ getting oxidized to form Cl_2. Further, recent studies have discussed the use of some low-cost substitutes, including urea[27,42-44] and related materials such as N-methyl urea, N-ethyl urea, triethylamine hydrochloride (Et_3NHCl), *etc.*[45], that help in the formation of favorable hydrogen bonds, in which the performance has yet to be developed. The use of GPEs such as acrylamides and polyamides (PAs) complexed with chloroaluminate-based ILs can be regarded as one of the most recent approaches for secondary RABs as they ensure increased safety and flexibility[30,46-48].

With the involvement of ILs, the redox reactions of a typical aluminum-ion battery (AIB) can be written as follows[49].

$$\text{At the anode: } 4Al_2Cl_7^- + 3e \leftrightarrow Al + 7AlCl_4^- \tag{1}$$

$$\text{At the cathode: } \text{Host} + 4nAl_2Cl_7^- + 3ne \leftrightarrow Aln\,[\text{Host}] + 7nAlCl_4^- \tag{2}$$

However, it is not only the electrolyte that affects the performance of secondary RABs; the anode and cathode also play a crucial role. Due to the incompatibility of Al metal with the electrolyte in primary batteries, different nanostructures of TiO_2 and MoO_3 have been used as Al^{3+} intercalation-type anodes. Nevertheless, Al metal has been the choice of the anode in the majority of secondary RABs with the operating mechanism of plating and stripping of the metal[50]. Different types of cathode materials involving layered structures or potential interstitial sites and diffusion pathways have been experimented with for secondary AIBs. The development began with the typical graphite electrode[15], and has evolved into including various other carbonaceous materials[51,52], transition metal compounds[5,53,54], Prussian blue[55] analogs, *etc.* However, the inability to achieve higher energy densities has led to the progress of studies with different composite electrodes. For instance, when graphene micro-flakes have been incorporated with Ni_3S_2 at a current density of 100 mAg^{-1}, an initial discharge capacity of 350 $mAhg^{-1}$ has been achieved. Yet, it has been dropped to a discharge capacity of around 60 $mAhg^{-1}$ after 100 cycles[56]. Different groups have carried out similar approaches[16,57], but most have incorporated carbonaceous materials in the composite. Other layered materials, including hexagonal BC_3[58] and MXenes[59,60] can be considered as further evolutions of cathode materials.

Although secondary AIBs have been gaining attention since 2011[58,59], their performance is far from emerging into commercial-level applications, leaving more room for development. Strategies such as increasing interlayer distance in layered materials to lower the energy barrier for ionic diffusion, along with the use of nanostructured materials and 3D structured materials, offer potential avenues for development[61,62]. Focusing on materials following conversion-type reactions rather than intercalation-type mechanisms would be some insights for further development. Further, an overall cell design with a good combination of all the cell components is of great importance.

Aluminum-air batteries

Aluminum-air batteries (AABs) are another type of aluminum-based battery on which a tremendous focus has been received. This type of battery is known to have a high theoretical specific energy of 4.30 $kWhkg^{-1}$, which is 5.20 $kWhkg^{-1}$ for lithium-air batteries, recognized as the highest of all metal-air batteries. In a typical AAB, the anode is Al, and the cathode is air-breathable, absorbing oxygen directly from the surrounding air[63]. The choice of electrolytes for AABs ranges around aqueous, organic, ILs, and solid-state, but aqueous alkaline electrolytes are frequently used. The electrochemical reaction in alkaline electrolytes can be given in[64]

$$\text{At the anode: } Al \rightarrow Al^{3+} + 3e^- \tag{3}$$

$$\text{At the cathode: } O_2 + 2H_2O + 4e^- \rightarrow 4OH^- \tag{4}$$

$$\text{Overall reaction: } 4Al + 3O_2 + 6H_2O \rightarrow 4Al(OH)_3 \tag{5}$$

Nevertheless, efforts with aqueous electrolytes have ended up being primary batteries because of their limited rechargeability due to parasitic H_2 evolution [Equation 6], leading to corrosion and passivation of the anode surface and accumulation of solid compounds on the surfaces of both electrodes inhibiting their exposure to the electrolyte. Rechargeable AABs have been reported when non-aqueous types of electrolytes are being used[65].

$$Al + 3H_2O + OH^- \rightarrow Al(OH)_4^- + \frac{3}{2}H_2 \tag{6}$$
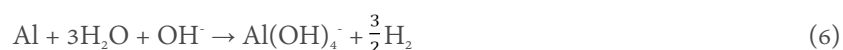
The performances of both the anode and the air-cathode are crucial factors for the overall functioning of the battery, and different microstructural aspects have been considered in their development. When considering the anode side, commercially available 2N5 and 4N grades of Al foils with purities of 99.5% and 99.99%, respectively, have been widely used. Notably, the grain size and the crystal orientation must be considered when fabricating the aluminum anode[66,67]. Finer grain sizes and single crystals with a (001) plane have been identified as the most favorable conditions for higher electrochemical performance with fewer corrosion rates, whereas equal channel angular pressing (ECAP) has been used to reduce grain size. As given in the electron backscatter diffraction (EBSD) technique in scanning electron microscopy (SEM), hydrogen evolution curves, and electrochemical impedance spectroscopy (EIS) in Figure 3, an optimum number of passes has been in ECAP decided to obtain finer grain size. The electrochemical performance is enhanced more when Al alloys are used instead of pure Al. Ga[68,69], Zn[70], and Sn[38] are the frequently reported alloyants. They have been suppressing corrosion by different mechanisms where Ga inhibits corrosion by forming an oxide layer, while Zn enhances corrosion resistance by increasing the potential for H_2 evolution[2]. Further, there are some approaches to modify the electrolyte[71,72] to suppress these unwanted reactions; additionally, different research studies have progressed towards the fabrication of corrosion inhibition coatings, which are applied either on pure Al or alloy anodes with the expectation of providing
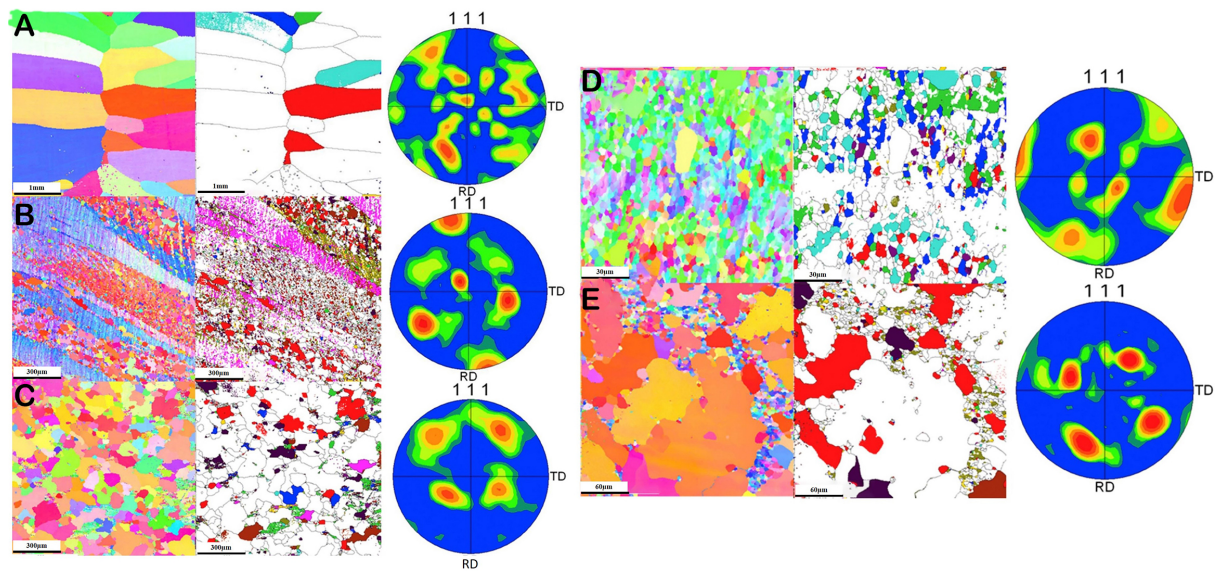
Figure 3. EBSD analysis of grain boundary and orientation maps after different ECAP passes (A) Cast, (B) three passes, (C) five passes, (D) seven passes, and (E) nine passes. Reproduced with permission ref.[66] copyright 2015 Elsevier.

barrier properties to both hydroxyl ions and water molecules. These strategies have been oriented to incorporating micro and nanostructures of carbonaceous, organic, and inorganic materials to achieve hydrophobicity[73-76].

The cathode is where the oxygen evolution reaction (OER) and the oxygen reduction reaction (ORR) respectively occur during the charging and discharging of the battery, and generally, it is composed of a catalyst, a current collector, and a gas diffusion layer[64]. Catalyst plays a significant role because these OER and ORR have sluggish reaction kinetics. Noble metals are the benchmarked type of catalysts for these reactions, but factors such as their high cost and low abundance have hindered their commercial application, leading to more room to research[77]. Carbonaceous materials, transition metal oxides (TMOs), sulfides and phosphides, transition metal dichalcogenides (TMDC), MXenes, and MOFs[78] have become the frequently experimented types of materials as catalysts. It is noteworthy that in a potential catalyst, along with adequate thermal, chemical, and mechanical stabilities, favorable surface reactions, mass, and electron transfers should be facilitated. Hence, having a porous structure ensures efficient mass transport with an increased number of active sites and accommodating discharge products. At the same time, good electrical conductivity should be maintained for an efficient electron transfer[78].

The utilization of numerous micro and nanostructures in their one (1D)-, two (2D)-, and three (3D)-dimensional arrangements has been an approach to accomplish the properties mentioned above. Tubular and rod-like structures, which come under 1D structures, have been incorporated in numerous studies. In research studies by Meng *et al.*[79], Yu e*t al.*[80] and Ma e*t al.*[81], carbon-based tubular or rod-like structures have been fabricated to be experimented with as air cathodes. As intrinsic carbon has always been outperformed by carbon incorporated with heteroatoms, the same strategy has been followed by them. Ma *et al.*[81] have used Fe_3C encapsulated in N-doped carbon fibers synthesized via a hybrid process of both hydrothermal and electrospinning techniques, while Meng *et al.*[79] have fabricated a mesh-type network containing Fe-N-C sites and clusters of Fe_3C via electrospinning. Once an AAB is assembled with an Al foil anode, a catalyst-coated carbon cloth cathode and a solid-state electrolyte, it demonstrates a specific capacity of 2,163.5 mAhg^{-1} at 10 mAcm^{-2}, while a comparable value of 2,002.2 mAhg^{-1} has been achieved at

the same current density as that by Meng *et al.*[79] using an Al foil anode and carbon paper loaded with the 4 M KOH electrolyte catalyst. A power density of 190.6 mWcm^{-2}, even higher than that of Pt/C having 142.1 mWcm^{-2}, has been achieved by using Fe_3C along with TiN in the form of quantum dots on CNTs[82]. This performance has been attributed to the reduction of energy barriers for ORR favored by the synergistic effect of Fe_3C-TiN. Using carbon nanofibers incorporated with Mn_3O_4 nanoparticles as the cathode and Al foil as the anode along with a solid-state electrolyte, flexibility in the battery has been achieved accompanied by a specific capacity of 1,273 mAhcm^{-2} at a current density of 2 mAcm^{-2} with a potential for application in wearable devices[80]. In contrast to the aforementioned, some studies have utilized inorganic-based structures to exclude carbon scaffoldings[83,84]. MnOOH nanorods decorated with CeO_2 and interconnected fibrous structures of Al_2O_3 are some examples, and the presence of interconnected porous microstructural cathodes can be highlighted for their enhanced ORR performance attributed to effective oxygen diffusion, high surface area, and structural stability.

Using different S and N co-doped carbon structures falling into the 3D categories (micro-rods, nanosheets, and 3D frameworks) synthesized via a template-assisted strategy, in the assembly of AABs, the 2D morphology has outperformed others, attributed to the sheet structures with high surface area enhancing the ion and electron transfer kinetics[85]. In the same way, numerous 2D structures have demonstrated their suitability as air cathodes where carbon has been selected as the base material in most studies. For example, using P-doped carbon dots incorporated in graphene sheet aerogel consisting of few-layered graphene achieves a power density of 157.3 mWcm^{-2}, slightly higher than that of Pt/C (151.2 mWcm^{-2}), which can be considered[86]. Moving further by combining the compositing and doping techniques in nanosheets, S and N co-doped graphene have been synergized with MnO_2, resulting in a specific capacity of 1,203.2 mAhg^{-1} at a current density of 5 mAcm^{-2}[87]. Following a similar approach, the use of Co_3O_4 grown in N-doped graphene oxide can be highlighted in a different study[88]. Other than nanosheets, flake-like structures of carbon have been successfully utilized in AABs as the catalyst for cathodic reactions, and N-doped carbon flakes with Fe single atoms, grown on a carbon cloth via a thermal reaction in an inert environment, have been able to exhibit a performance with a stable discharge voltage of 1.5 V over 8 h at 1 mAcm^{-2}[89]. Moreover, different hierarchical structures of Mn oxides have been grown on graphene by varying the amplitude of ultrasonication during the synthesis process, and multilayer spheres, nanorods, and nanowires, as given in Figure 4, have been obtained where graphene with nanorods and nanowires of MnO(OH) [Figure 4B] has been identified as the best way to promote ORR closely aligning with the commercial 20% Pt/C catalyst from Figure 4E and F[90].

Even though 2D morphology has been preferred in some studies[85], some successful attempts have been made to design better-performing air cathodes with 3D morphology. A carbon-based catalyst has been fabricated by intercalating different molar compositions of Co ions into the interlayer spaces of MnO_6 to obtain Co-MnO_2. The subsequent dispersion of Co-MnO_2 in conductive carbon black and testing in a battery set up with Al foil as the anode and urea containing $AlCl_3$ as the electrolyte, 40% molar composition of Co in Mn has been identified as the optimum[91]. Microstructure, specific surface area, and the rich redox chemistry of Mn and Co have been considered major reasons for this performance enhancement. Honeycomb-like carbon has been known to provide channels for fast ion transportation and active reaction sites. Attributing these properties, Co_3Fe_7-Fe_3C anchored onto an N-doped honeycomb-like carbon has been able to show a power density of 210 mWcm^{-2} at a current density of 286 mAcm^{-2} and the performance has been reported to be higher than the value obtained for Pt/C (180 mWcm^{-2} at 273 mAcm^{-2}) when tested in 4 M NaOH electrolyte with an Al-Mg-Sn alloy anode.
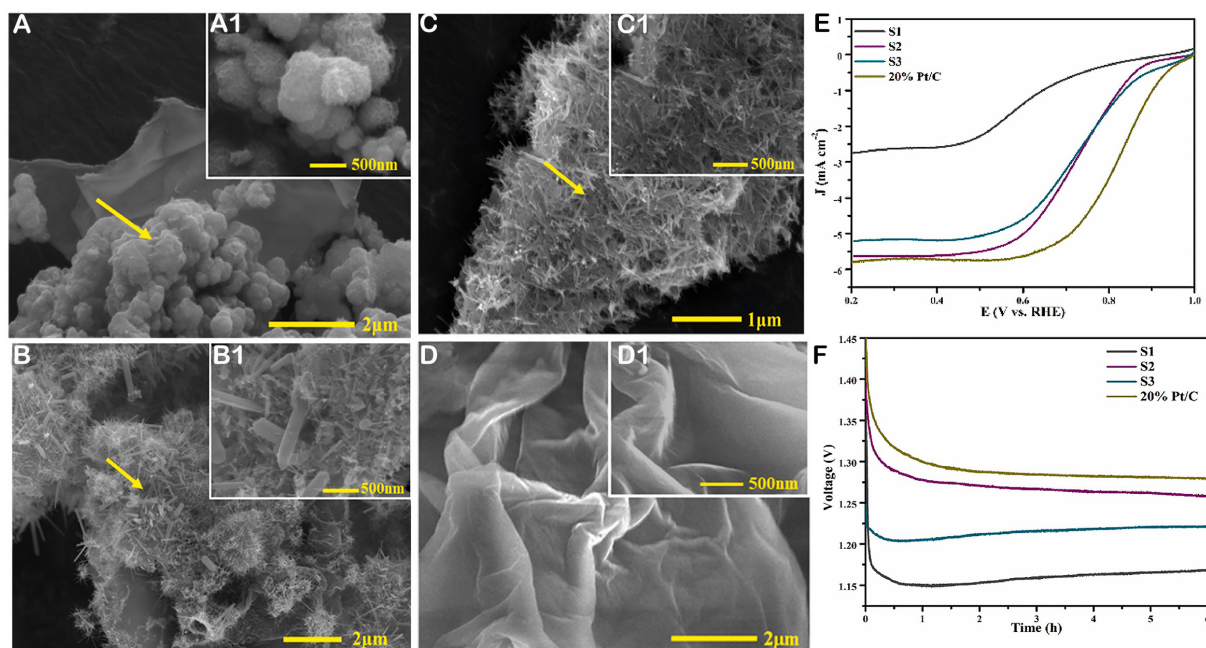
Figure 4. SEM images of graphene with hierarchical structures of (A) Mn oxides – multilayer spheres, (B) nanorods and nanowires, (C) nanowires, (D) graphene oxide, (E) LSV curves, and (F) galvanostatic discharge curves at 30 mAcm^{-2}. Reproduced with permission ref.[90] copyright 2023 Elsevier.

From Figure 5A-H, the honeycomb-like structures derived from soybean roots are an insightful utilization of biomass[90]. Moreover, in a different study, Fe-enriched N-doped 3D hierarchical carbon derived from a MOF has been utilized as the catalyst, and the porous structure with more active sites from doped N in the MOF has enhanced the even distribution of Fe, preventing the aggregation of inactive Fe. This has been ascribed to strong interactions between Fe, N, and C in the structure. Further, providing a feasible solution to solid waste, this study has used Al beverage cans as the anode (alloy of Al and Fe) in which comparable results have been achieved in terms of discharge capacities, respectively, with 1,173 and 1,920 mAhg^{-1} for Al can and pure Al foil anodes at a current density of 20 mAcm^{-2}[92]. From further, synergy in incorporating structures of different dimensions into 3D architectures has been reported as a favorable approach to enhance electrocatalytic performance and fabrication of a catalyst comprising clusters of ultrathin Co_3O_4 nanosheets anchored on N-doped CNTs, which are ultimately grafted on a 3D graphene standing on a Ni foam substrate, as indicated in Figure 5I, can be reflected. In the synthesis procedure, hydrothermal treatment followed by calcination was utilized to synthesize Co_3O_4 structures, while graphene and CNTs were fabricated via chemical vapor deposition (CVD). This material has been used in the assembly of an AAB as a binder-free cathode, and the assembled battery with an aluminum anode and 2 M KOH electrolyte has resulted in a specific capacity of 483.80 mAhg^{-1} while Pt/C electrode resulted in 361.74 mAhg^{-1}. The electrocatalytic activity can be further highlighted in Figure 5J and K with the linear sweep voltammetry (LSV) curves and discharge curves, respectively[31].

Moreover, inorganic 3D structures, including perovskites, have been experimented with in AABs as air cathode materials, and $La_{0.4}Sr_{0.6}Co_{0.7}Fe_{0.2}Nb_{0.1}O_3$-δ[93] and $La_{0.75}Sr_{0.25}MnO_3$[94] are some examples. Chemical composition and flexible crystal structure facilitating adjustable physicochemical and electronic properties have been reported as the main reasons for the applicability of perovskites. In the synthesis of $La_{0.4}Sr_{0.6}Co_{0.7}Fe_{0.2}Nb_{0.1}O_3$-δ perovskite, two methods, sol-gel and solid phase (ball-milling), have been exploited. According to the comparison of their electrochemical performance, perovskites synthesized via
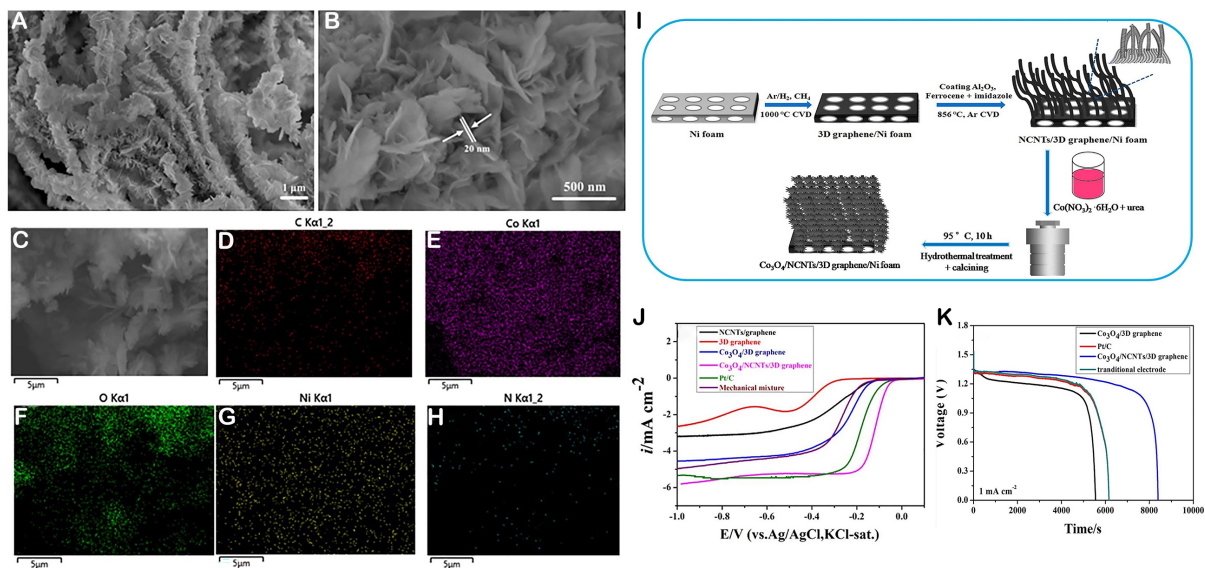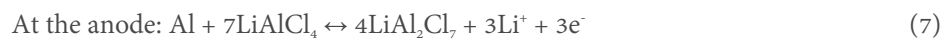
Figure 5. (A and B) SEM images of Co_3O_4/NCNT's/3D graphene, (C) selected area for elemental mapping; elemental mapping of (D) C, (E) Co, (F) O, (G) Ni, and (H) N, (I) schematic diagram of the synthesis procedure, (J) LSV curves of different cathodes on a rotating disk electrode in O_2 saturated 0.1 mole KOH solution at a rotation of 1,600 rpm with a scan rate of 5 mVs^{-1}, and (K) discharge curves of the coin air batteries at a current density of 1.0 $mAcm^{-2}$. Reproduced with permission ref.[31] copyright 2020 Elsevier.

sol-gel techniques (power density of 68 $mWcm^{-2}$ at 80 $mAcm^{-2}$) have outperformed the perovskite by ball-milling (power density of 56 $mWcm^{-2}$ at 70 $mAcm^{-2}$), due to the availability of high specific surface area inherited with the porous structure in the sol-gel method perovskite[93]. On the other hand, $La_{0.75}Sr_{0.25}MnO_3$ perovskite has indicated a particular capacity of 1,084 $mAhg^{-1}$ at 5 $mAcm^{-2}$ current density[94]. Even though not much work related to perovskites is in the public domain when compared to carbon-based catalysts, with substantial work, a better-performing and durable catalyst can be developed.
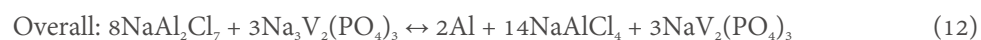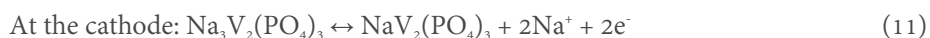
HYBRID LI/AL BATTERY DEVELOPMENT

Despite Al being able to exchange three electrons during the electrochemical process due to its multivalency compared to one electron in Li, strong electrostatic interactions between Al^{3+} and the cathode have been a reason for sluggish reaction kinetics[95]. Therefore, scientists have paved their thinking towards bypassing the requirement of efficient insertion/extraction of Al^{3+} at the cathode by developing the hybrid battery system. In the study by Sun *et al.*[26], an aluminum hybrid battery has been developed in which an aluminum anode has been used along with a $LiFePO_4$ cathode, and therefore, reversible Al deposition/stripping and Li intercalation/deintercalation occur respectively. In this hybrid battery, IL EMIC with $AlCl_3$ has been chosen as the electrolyte. In this slightly acidic system, Li^+ is extracted from the $LiFePO_4$ cathode, but the performance has been further improved by adding Li salt such as $LiAlCl_4$ to this electrolyte. The formation of Al-Li alloy has been excluded due to the high potential for Al deposition compared to alloy formation in an acidic medium[26].

$$\text{At the anode: } Al + 7LiAlCl_4 \leftrightarrow 4LiAl_2Cl_7 + 3Li^+ + 3e^- \tag{7}$$

$$\text{At the cathode: } FePO_4 + Li^+ + e^- \leftrightarrow LiFePO_4 \tag{8}$$

$$\text{Overall: } Al + 7LiAlCl_4 + 3FePO_4 \leftrightarrow 4\ LiAl_2Cl_7 + 3LiFePO_4 \tag{9}$$

In a different study[96], the current collector used by Sun *et al.*[26], Cu, has been replaced with pyrolytic graphite on the cathodic side to withstand corrosion. $LiFePO_4$ has been cast on this pyrolytic graphite current collector, and LiCl has been used as the source of Li salt instead of $LiAlCl_4$. The study has resulted in a gravimetric capacity of 129 mAhg^{-1} at a current density of 80 mAg^{-1} along with an operating voltage of 1.3 V and a capacity retention of 83.4% upon the completion of 400 cycles.
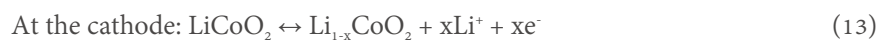
Moreover, further developments of this hybrid battery concept have oriented to Na instead of Li, considering the availability of limited resources of Li, which is already a concern in attempts to develop alternative batteries for LIBs. In a potential example, along with an aluminum anode, $Na_3V_2(PO_4)_3$ has been used as the cathode with the addition of $NaAlCl_4$ dissolved in EMIC and $AlCl_3$ electrolyte. Reversible Al deposition/stripping in the anode and extraction/insertion of Na^+ during the electrochemical process can be given in[97]

$$\text{At the anode: } 4NaAl_2Cl_7 + 3Na^+ + 3e^- \leftrightarrow Al + 7NaAlCl_4 \tag{10}$$

$$\text{At the cathode: } Na_3V_2(PO_4)_3 \leftrightarrow NaV_2(PO_4)_3 + 2Na^+ + 2e^- \tag{11}$$

$$\text{Overall: } 8NaAl_2Cl_7 + 3Na_3V_2(PO_4)_3 \leftrightarrow 2Al + 14NaAlCl_4 + 3NaV_2(PO_4)_3 \tag{12}$$

Even though this hybrid approach has been taking advantage of both systems where aluminum anode suppresses the dendrite formation and the presence of Li^+ and Na^+ exhibiting good capacities and cycling performances, there are only a few studies in the public domain thus far. Further, although these studies validated the hybrid aluminum battery concept, they have not been able to perform closer to the current state-of-the-art LIBs. However, this concept can be very beneficial in terms of safety and earth abundance and, hence, is worthy of further development.

One pathway to improve the performance can be the resolving of issues related to the low electronic conductivities of $LiFePO_4$ and $Na_3V_2(PO_4)_3$[98,99]. Identifying other possible compounds to replace or carrying out different modifications to these same materials are two possible options. Utilizing micro or nanostructures, encapsulating materials with conductive layers such as carbon or polymers, compositing with metal oxides, or doping with heteroatoms are some potential directions for future work.

In addition to hybrid batteries, Al has been utilized in LIBs in some approaches where more than one metal ion has been used. With the use of these multiple metal ions, a synergistic effect has been expected in aspects of fast diffusion of monovalent ions and high capacity due to the involvement of multivalent ions. In this setup, Li^+ has de-intercalated from the $LiCoO_2$ cathode and has shuttled towards the aluminum anode to produce AlLi alloy while charging and reverse to happen while discharging[100].

$$\text{At the cathode: } LiCoO_2 \leftrightarrow Li_{1-x}CoO_2 + xLi^+ + xe^- \tag{13}$$

$$\text{At the anode: } Al + Li^+ + e^- \leftrightarrow AlLi \tag{14}$$

$$\text{Overall: } LiCoO_2 + xAl \leftrightarrow xAlLi + Li_{1-x}CoO_2 \tag{15}$$

Al has been used as an anode and is currently a collector in this arrangement. Hence, the use of Cu foils for current collectors, binders, and steps, including mixing and baking, has been omitted. These provide

additional advantages, including reducing fabrication costs and getting rid of potential short circuits caused by the oxidation and dissolution of Cu. By utilizing the same concept as[100], a different study has used a λ-MnO_2 anode and $LiAlCl_4$ in EMIC and $AlCl_3$ electrolyte to obtain a discharge capacity of 94 mAhg^{-1}[101]. However, it has dropped down to 54 mAhg^{-1} after 50 cycles following a similar trend as in the work of[100] in which the initial capacity reported as 160 mAhg^{-1} has subsequently dropped down significantly after 70 cycles.

The rapid fading of the capacity in these metallic aluminum anodes is attributed to the irreversible lithiation with the oxide layer leading to the formation of Li_xAlO_y, pulverization caused by volume changes after extended cycling and trapping of Li in Al[102,103]. In addition, these Al foil electrodes have not been able to provide considerable coulombic efficiency. Despite the aforementioned problems, studies in this context have been preceded due to the high theoretical capacity and the potential of lithiation/delithiation by using Al[104]. In contrast to other elements, alloying with Al has several advantages including a significantly lower percentage of volume change of ~96% (320% for Si[105,106] and 260 % for Sn)[107] during lithiation/delithiation and a Li diffusion coefficient of 6.0×10^{-10} $\Omega^{-1}cm^{-1}$ higher than that of bare lithium metal (5.69×10^{-10} $\Omega^{-1}cm^{-1}$)[108]. The forming of a passivation oxide layer has also been considered an advantage as it provides a stable concealment of the alloy from moisture[109].

Therefore, pre-lithiation techniques have come into play, and electrochemical lithiation is the frequently employed method in this context. Electrochemical and mechanical strategies have been frequently used as lithiation techniques and in a typical setup of electrochemical lithiation, Al and Li foils separated by a polypropylene membrane have been serving as the cathode and anode, respectively. Using 1 M $LiPF_6$ in a 1:1 volume ratio of ethylene carbonate (EC) and ethyl methyl carbonate as the electrolyte, the coin cell has been discharged for 12 h at a current density of 0.06 mAcm^{-2} to accomplish lithiation[109]. Alternatively, in a simple electrolyte-mediated mechanical rolling method enabling the formation of a unidirectional lithiation with a Li concentration gradient, 5 µL of an electrolyte containing 1.3 M $LiPF_6$ in EC, diethyl carbonate, and fluoroethylene carbonate (FEC) in different proportions has been placed in between the plates of Al and Li of 14 mm diameter before the application of a pressure of 62 kPa[110]. In both methods, the resultant alloy has been subsequently washed with dimethyl carbonate to discard any residual matter before further use as the anode material in LIBs. Even though four main phases, β-LiAl, Li_3Al_2, $Li_{2-x}Al$, and Li_9Al_4, have been identified in Al-Li alloy due to the high reactivity of Al with Li, room temperature lithiation techniques have been restricted only to β-LiAl with a composition variation in the range of 47-56 at%. During the lithiation, the lattice parameter of 4.05 Å in Al with a face-centered cubic has changed to 6.37 Å in β-LiAl, attributing to the previously mentioned volume expansion of ~96 %[104]. β-LiAl has been known to have a theoretical specific capacity of 993 mAhg^{-1} (calculated for ideal 50:50 composition), which can be considered as more than two times that of graphite, which is the typical anode material used in LIBs[100].

With the use of pre-lithiation, the cyclability has been reported with significant improvements. With the employment of a $LiNi_{0.8}Co_{0.1}Mn_{0.1}O_2$ cathode, the pre-lithiated aluminum anode has indicated a discharge capacity of 162 mAhg^{-1} after 400 cycles with a capacity retention of 90% in contrast to a pristine aluminum anode in which its discharge capacity has dropped below 50 mAhg^{-1} even before running 100 cycles[103]. The inability to achieve the theoretical discharge capacity in the above study has been continued with a different study as well where β-LiAl anode material fabricated via electrochemical lithiation has been tested in a battery using commercially purchased $LiFePO_4$ cathode and a porous polymer separator using $LiPF_6$ electrolyte[110]. The SEM image in Figure 6 depicts the surface and cross-sectional view of the formed β-LiAl layer, and according to the obtained potentiostatic charge counting data, it has been composed of 53.7 at% of Li and 46.3 at% of Al. Although the theoretical capacity relevant for this composition is 1,152 mAhg^{-1}, it
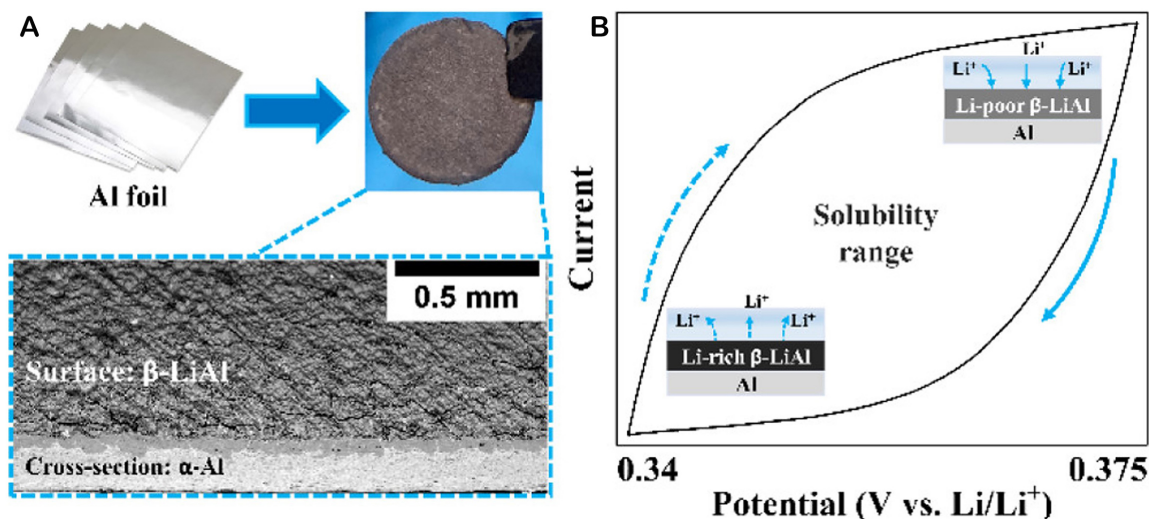
Figure 6. SEM images of partially lithiated Al foil and the solubility range of Li. Reproduced with permission ref.[111] copyright 2023 American Chemical Society.

has been unachievable. Further, the difference in the diffusion of Li in the two phases [lithium-rich (β-LiAl) and lithium-poor (α-Al)] leading to the trapping of Li has been identified as a crucial factor affecting the cycling performance. Hence, in the same study, the lithiation/delithiation of the β-LiAl layer was carried out without initiating any phase changes by maintaining the voltage window around 0.34-0.38 V (*vs.* Li/Li⁺). This approach has retained 96% of the capacity for more than 500 cycles at a current density of 0.1 mAhcm⁻² once paired with a commercially available cathode[105,111].

Although pre-lithiation approach has enhanced the cycle performance compared to free-standing Al foil anodes, many issues are yet to be addressed. Major concerns include the unscalability of the electrochemical lithiation method from the lab scale to the industrial level, and the inhomogeneity of the lithiation due to poor wettability of Al[112]. On the other hand, poor cyclability has been an issue where even though it has been expected that pulverization during cycling might be mitigated due to lower volume expansion compared to other probable elements for alloying, practically, Al has shown the worst cyclability in foil geometry[113].

Hence, research is ongoing to optimize the utilization of Al in LIBs. Fabrication of nanostructures containing Al is one approach. Nevertheless, the fabrication of nanostructured aluminum has proven challenging due to its low Mohs hardness, affecting the feasibility of the top-down approach, and its high chemical reactivity, posing challenges for the bottom-up approach in nanoparticle synthesis. Despite that, there are remarkable efforts in which techniques such as thermal plasma evaporation[114], wet chemical synthesis[115], mechanical rolling, and plasma-enhanced CVD (PECVD)[116] have been utilized. The use of carbonaceous materials to scaffold the Al nanostructures has been widely utilized. A nanocomposite with Al nanoparticles synthesized via thermal plasma evaporation and condensation followed by dispersion with graphene oxide in tetrahydrofuran (THF) via ultrasonication to get the expected nanocomposite has been combined with carbon black and polyvinylidene fluoride (PVDF) before coating on a Cu foil. An assembled battery with this nanocomposite as the anode and a Li foil as the cathode separated by polypropylene film in an electrolyte of 1 M LiPF₆ in a 1:1 volume ratio of EC, diethyl carbonate, and FEC has exhibited a discharge capacity of 1,041 mAhg⁻¹ at a current density of 500 mAg⁻¹ even after 500 cycles[114]. The achievement of a volumetric capacity of 1,089 mAhcm⁻³ at 3 mAcm⁻² current density for 20,000 cycles has been a significant

improvement in which the anode was fabricated by repeated folding and rolling of an Al foil along with a Sn foil using a rolling machine, where Sn has subsequently removed via selective chemical etching. The final nanocomposite has been fabricated by dispersing these Al nanosheets with graphene[116].

Alloying Al with other elements is the second approach, and it has been experimented with to aid the initiation of atomic defects and enable transformations in the crystalline structure of LiAl. Further, the involvement of these binary and ternary alloy systems has reduced volume expansion during lithiation/delithiation. Two different studies using a binary system of Al and Cu[117] and a ternary system of Al, Mn, and Si[118] separately can be considered as example studies. Upon the assembly of a complete cell with a LiFePO$_4$ cathode, the Cu-Al anode has been able to retain nearly 88% of the discharge capacity for more than 200 cycles. On the other hand, only 70 cycles retained 90% of the discharge capacity when the Li$_x$AlMnSi anode was tested with a LiFePO$_4$ cathode, even though it depicts a significant improvement compared to the β-LiAl cathode.

Another approach involves surface modification and coating the Al foil with a poly(ethylene oxide)-based polymer to create a porous, stable 3D nanostructure, with the forming β-LiAl as an example[105]. In a different study, the anode was fabricated using a Cu current collector coated with a thin film of Al and subsequently encapsulated with four CVD-grown graphene layers. The idea of encapsulation by graphene is to extend cyclability by preventing pulverized Al nanoparticles from detaching from the anode. It has been able to indicate ~900 and ~780 mAhg^{-1} discharge capacities after 500 and 1,000 cycles[119].

Accordingly, different approaches are under experiment as the current state of the art is not up to expected excellence. Therefore, it can be concluded that the use of Al as an anode material in LIBs is still progressing and there is more room to research. Furthermore, it can be worth experimenting with as it can be advantageous in numerous aspects, omitting the unsafe dendrite formation, reducing the cost of preparation, and improving the recyclability of the degraded battery, making it more environmentally friendly.

OVERALL PROGRESS OF NON-AQUEOUS RABS
Anode
Historically, the preference among researchers for anodes has predominantly leaned towards utilizing Al foil[120,121]. However, persistent challenges, including the formation of passivation films, aluminum dendrites formation, pulverization, and electrochemical corrosion, have posed significant hurdles. Effectively overcoming the critical issues has become a demanding priority, necessitating a thorough exploration of alternative and stable anode options. The subsequent discussions will focus on the details of various materials that serve as potential alternatives for anodes.

Al & Al alloy-based anode materials
Aluminum is a promising battery anode due to its high theoretical voltage and specific energy, with efforts focused on RABs. Challenges include dendrite growth and electrode disintegration, which are addressed by applying a protective Al oxide layer[122,123]. However, issues persist, including an insulating native oxide layer hindering Al plate/stripping and high-bandgap oxide affecting electron and ion flow. Research explores solutions such as novel electrolytes, alloy anodes, and surface modifications[124,125]. Recent progress involves chemically treating Al foil, creating a conductive layer, and limiting native oxide, leading to lower over potential during Al plating/stripping. Treated Al shows promise for improved battery cycle life. Innovative methods, such as deep eutectic solutions, aim to overcome oxide layer challenges and enhance AIB electrochemical performance[126].

Aluminum faces challenges as an energetic material in aqueous and non-aqueous solutions due to oxide coating, slowing dissolution, and shifting potential. Self-corrosion reduces Coulombic efficiency (CE) on discharge and standby mode capacity. Using an alternate anode increases cell lifespan but compromises energy density due to Al^{3+} ions' intercalation mechanism in TiO_2[125-128]. Alloys with activator elements (Sn, Ga, Mg) show potential but require modification due to non-coulombic loss. Zirconium oxide (ZrO_2) nanoparticles improve metallurgical and electrochemical characteristics when added to Al alloys by providing benefits such as grain refinement, enhanced corrosion resistance, and improved electrochemical stability. Nano-ZrO_2-reinforced Al-Mg-Sn-Ga alloys have exhibited improved anode performance, reducing energy dissipation in RABs[127,129]. Al-copper alloy lamellar heterostructures enhance Al-ion electrochemical reversibility, achieving dendrite-free Al deposition during cycles. The eutectic $Al_{82}Cu_{18}$ alloy electrode maintains the stripping/plating of Al at low overpotential for 2,000 h. In an RAB full cell, the $Al_{82}Cu_{18}$ anode paired with the Al_xMnO_2 cathode achieved a specific energy of 670 Whkg⁻¹, an initial discharge capacity of 400 mAhg⁻¹ with 83% retention after 400 cycles.

In the exploration of aluminum as a potential anode material for LIBs, it has gained attention as a typical alloy-type anode material in the[10] due to its high theoretical capacity, cost-effectiveness, and average potential plateau during lithium plating[12,130,131], minimizing dendrite formation and addressing safety concerns in lithium electrodes at room temperature. In such a work, Al thin films with varying thicknesses ranging from 0.1 to 1 μm have been deposited *via* thermal evaporation techniques and have demonstrated high capacities approaching 1,000 mAhg⁻¹[132]. However, they have resulted in unsatisfactory first-cycle CE and capacity losses throughout the cyclability test, attributed to significant strain induced by volume changes. Despite these challenges, another related work has highlighted the potential viability of Al as an anode material for LIBs where a foil of aluminum with a 21 μm thickness has been utilized in a half cell along with lithium serving as the counter/reference electrode. Their investigation has mainly focused on the effect of the composition of an electrolyte on cycling performance[133]. This half-cell combination has displayed optimal performance during the cycling test in a 1 M $LiPF_6$ solution containing a combination of FEC (30 vol%) and ethyl-methyl carbonate (EMC, 70 vol%) along with vinylene carbonate (VC, 3 wt%) and ethylene sulfite (ES, 2 wt%) as other additives. It has been able to achieve a considerable reversible capacity of 967 mAhg⁻¹ along with the retaining of 80% of the capacity after 15 cycles at a current density of 1 mAcm⁻²[134]. The study revealed that the incorporation of a small quantity of VC has improved capacity retention significantly, and further replacing EC with FEC along with additional ES has resulted in a more pronounced advancement in cycling stability. The synergistic effect imparted by the above-mentioned functional electrolytes has facilitated the formation of an efficient layer of inorganic and elastic organic polymer on the surface of the Al electrode, mitigating the adverse effects of volume changing and thereby boosting the cyclic stability. Notably, aluminum can attain an enhanced specific capacity (993 mAhg⁻¹) accompanied by a comparatively lower variation in volume (97% volume expansion for Li-Al) while other potential metallic materials such as Sn, Zn, and Sb have specific capacities of 994, 410, 660 mAhg⁻¹ and volume expansions of 260% (for $Li_{4.4}Sn$), 98% (for Li-Zn) and 147% (for Li_3Sb), respectively.

Nonmetallic-based anode materials
Exploration of nonmetallic materials as anodes in RABs has been limited in current research. Initial investigations considered TiO_2 due to its low intercalating voltage of Al^{3+} ions in aqueous aluminum batteries, although its utilization in non-aqueous RABs remains unreported. Graphite has surfaced as a promising candidate for the anodes in aluminum batteries, as illustrated by[135], the success of a dual-graphite battery featuring excellent cycling stability and discharge voltage plateaus. Comparable achievements were observed in graphite-graphite RABs, demonstrating performance on par with those employing aluminum as the anode. The introduction of a lightweight, corrosion-resistant nitrogen-doped

carbon rod array (NCRA) as a nonmetallic anode showcases extended cycle life compared to Al foil. Despite these promising developments, the realm of nonmetallic anodes in RABs remains underexplored. To further expand material options, it is essential to investigate additional alternatives. Directed attention towards the development of suitable anode materials for non-aqueous RABs is crucial to achieving breakthroughs in both safety and performance. Research on anodes in RABs based on nonmetallic materials is significantly underexplored despite most studies focusing on cathodes and electrolytes. The development of a stable RAB system hinges crucially on advancements in anode development, emphasizing the need for more attention to be directed toward research in this area[136,137].

Cathode

In addition to the high availability of resources and easy affordability, non-aqueous RABs distinguish themselves from traditional batteries following rocking-chair mechanisms such as LIBs or sodium-ion batteries (SIBs) by involving multiple sorts of active ions in both processes at the anode and cathode. Consequently, the kinetics of electrodes at both positive and negative terminals become a crucial consideration. Ideal cathode materials for RABs should exhibit the following properties: (1) effective electronic and ionic conductivity; (2) elevated redox potential and specific capacity for enhanced energy density; (3) high reversibility in the reaction process to ensure robust cycling stability; (4) excellent thermodynamic and chemical stability across the entire voltage range; and (5) well-balanced electrode kinetics between the two terminals.

Based on energy storage mechanisms, cathodes in acidic $AlCl_3$ based electrolytes can be classified into three types: reversible intercalation/deintercalation reactions, adsorption/desorption reactions, and conversion reactions. The first type further distinguishes between the intercalating $AlCl_4^-$ and Al^{3+}. Electrode materials relying on intercalation mechanisms typically limit the electron transfer number to 1 but not more, leading to constrained battery energy density. In contrast, electrochemical conversion reactions overcome limitations related to both phase changes and alterations in the structure of the material used to compose the electrode during the charge and discharge of the cell. This has allowed the reversible execution of multiphase conversion reactions, potentially storing more than one electron per single mole of the conversion-type material. Consequently, non-aqueous RABs utilizing the conversion mechanism hold the promise of achieving high-energy capacities through these multi-electron redox reactions.

Carbon-based cathode materials

Carbon, prized for its exceptional electrochemical properties, high conductivity, high natural abundance, and modest prices, stands as a prominent material for energy storage in Energy Storage Systems (ESSs)[138]. Notably, porous carbons, activated carbons, graphitic carbons, and amorphous carbons have significantly propelled advancements in LIBs, Li-S batteries, and other ESSs. However, in RABs, the carbon-based cathode has encountered challenges, as evidenced by a notable report in 1988 introducing an Al/graphite battery using an RTIL electrolyte achieving an average operating voltage of 1.7 V and stable cycling, where challenges such as Cl_2 gas evolution limited further development[139,140]. Research efforts have explored alternative approaches, including the use of electrochemically fluorinated natural graphite (FG) and commercial carbon paper as cathode materials. While FG demonstrated high discharge capacity and coulombic efficiency, concerns remained regarding charge/discharge plateaus[141]. The utilization of commercial carbon paper addressed some issues, demonstrating practicality and viability with an intermediate voltage plateau at 1.8 V. Despite achieving good discharge capacity, challenges persisted at the high value of current densities. In the pursuit of efficient and cost-effective alternatives, researchers have explored alkali chloroaluminate ($NaCl$-$AlCl_3$) electrolytes, achieving an enhanced discharge capacity of 190 mAhg^{-1} and at a tremendously high current density such as 4,000 mAg^{-1}, an excellent cycling performance has been observed. However, the high-temperature operation raised practicality concerns.

Innovative approaches, such as the creation of monolithic aligned[23] few-layered graphene sheets within 3D graphitic foam (3DGF), have yielded positive outcomes. Despite challenges associated with the impact of large ion insertions on rate performance, efforts to enhance the graphite interlayer spacing have resulted in improved electrochemical performance. Both commercially expanded[142] graphite cathodes and graphitized EG3 K (EG = expanded graphite) cathodes have demonstrated high capacity and rate capability, effectively addressing issues faced by conventional graphite-based AIB systems[25]. A rechargeable AIB featuring a film of SP-1 natural graphite flakes (NG) with a PVDF binder as the cathode exhibits distinct discharge voltage plateaus ranging from 2.25-2.0 V and 1.9-1.5 V[143,144]. The graphite cathode displays a significantly improved specific capacity of up to 110 mAhg^{-1}, achieving a CE of approximately 98% at a current density of around 99 mAg^{-1}. Notable, charge-discharge cycling at a current density of 660 mAg^{-1} reveals exceptional stability, with minimal capacity decay observed over an impressive 46,000 cycles, maintaining a CE of over 99%.

In searching for high-capacity carbon cathodes, Panya *et al.* synthesized low-cost and highly defective mesoporous activated carbon from coconut shells followed by activation with KOH and investigated its cathodic performance against RABs[32]. This study reveals that activation with a higher KOH:C ratio can result in more and larger mesopores with high surface area, which can easily intercalate large-sized AlCl$_4^-$. This good capacity is ascribed to the massive number of mesopores [Figure 7A-C] with a high surface of 2,686 m^{2}g^{-1}. The produced carbon, activated with a ratio of 5:1 (KOH:C), delivered a discharge capacity of 150 mAhg^{-1} at 0.1 A [Figure 7D]. In this case, the adsorption-desorption process was the primary charge storage mechanism, as no oxidation reduction peak was found in the cyclic voltammetry (CV) data [Figure 7E] but the cycling stability was stable up to 1,500 cycles at 1 Ag^{-1} [Figure 7F].

Transition metal oxide based cathode materials
Along with carbonaceous materials, Transition metal oxides (TMOs) have been effectively utilized as suitable candidates to fabricate cathodes in rechargeable batteries, offering sufficient room for intercalating and subsequent deintercalation of relevant ions throughout the cycling process. Beyond batteries, these materials have demonstrated efficient performance in various applications, including photocatalysis, photochemical reactions, and dye-sensitized solar cells, attributed to their advantageous features such as increased surface area providing more room for reactions and short solid-state diffusion pathways. Given that RABs are trivalent-ion batteries[136], thanks to their multivalent nature, TMOs emerge as promising candidates for cathode materials due to their ability to accommodate more electrons. The initial exploration of TMOs in RABs was pioneered by[14,145] who employed l-Mn$_2$O$_4$ as a cathode material in AlCl$_3$/EMIC Cl electrolyte, achieving a notable discharge capacity and energy density surpassing conventional LiC$_6$-Mn$_2$O$_4$ systems. Despite challenges, such as slow diffusion and rigid Al^{3+} ion fixation, researchers have investigated strategies to enhance the performance of TMOs[146-148]. For instance, uniform V$_2$O$_5$ nanowires were synthesized and utilized as a cathode, showing a high discharge capacity, albeit with certain drawbacks such as poor coulombic efficiency. Researchers further developed Ni foam-supported Ni-V$_2$O$_5$ cathodes, emphasizing the reactivity of V$_2$O$_5$ toward Al metal in acidic RTIL electrolytes. Additionally, the reversible storage of Al^{3+} cations in V$_2$O$_5$ nanowires has shed light on intercalation and phase-transition reactions. Despite these advancements, challenges persisted, including issues with CE and limited cycle life, particularly in aqueous electrolytes[147,148].

Vanadium oxychloride (VOCl), characterized by its layered structure, emerges as a prospective cathode material for RABs due to its substantial interlayer spacing and impressive theoretical capacity[149]. This study marks the inaugural utilization of VOCl as the cathode material for RABs with a comprehensive investigation into its electrochemical performance and underlying mechanisms[150]. Figure 8A and B illustrates the distribution of V^{3+} ions within the layered orthorhombic structure, where these ions are
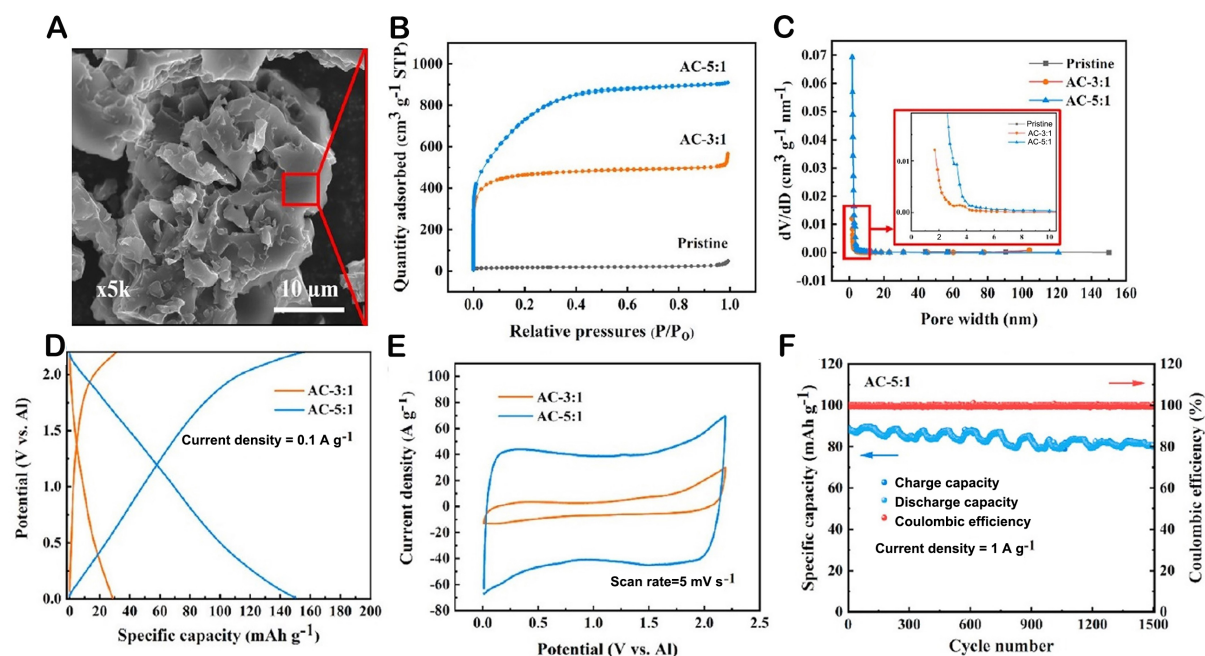
Figure 7. (A) SEM image of AC-5:1 activated carbon, (B) N_2 isotherms, (C) pore size distribution of different activated carbon, (D) galvanostatic charge/discharge (GCD) curves, (E) cyclic voltammograms (CV curves), and (F) cycling stability of activated carbon cathodes fabricated from AC-3:1 and AC-5:1 material. Reproduced with permission ref.[32] copyright 2022 Elsevier.

centrally located, forming a bilayer network structure. The refined lattice parameter before and after has been changed and observed. Field emission SEM (FE-SEM) images of the as-prepared VOCl and VOCl/ graphene materials show the VOCl presents a long flake-like morphology with dimensions 30μm in length, 2 μm in thickness, and 10 μm in width. After ball milling with graphene, the long flake structure was destroyed and formed VOCl nanoflakes[151]. Figure 8C-F indicates that the redox reaction is related to the $AlCl_4^-$ interaction/deintercalation of the VoCl phase. The first charge VOCl cathode demonstrates a commendable reversible discharge capacity of 124.7 mAhg^{-1} attributed to the deintercalation of $AlCl_4^-$ and subsequent intercalation of Al^{3+}[16]. Nevertheless, the discharge capacity diminishes to 41.5 mAhg^{-1} after 100 cycles, primarily due to irreversible intercalation/deintercalation of $AlCl_4^-$ during cycling; the electrochemical capacity of the VOCl cathode in RABs is chiefly governed by Al^{3+} intercalation/ deintercalation post the initial cycle. Additionally, the study reveals the absence of noticeable lattice expansion when $AlCl_4^-$ or Al^{3+} is intercalated into the interlayers of VOCl[152,153].

Explorations have extended to tunnel-structured VO_2 nanorods, showcasing stable electrochemical performance in RTIL electrolytes. The long-term discharge is observed to decay in a capacity of 124.7 to 60 mAhg^{-1}. However, challenges such as the potential trapping of intercalation products within VO_2 tunnels were observed. Anatase TiO_2 nanotube arrays (TiO_2-NTAs) were also investigated as cathode materials for RABs[17], revealing reversible intercalation/deintercalation of Al^{3+} cations. However, challenges arose concerning the formation of Al oxidative layers and other corrosion products in aqueous systems. While TMOs such as V_2O_5, V_2O, and TiO_2 have been reported to exhibit higher capacity in RABs than cathodes synthesized using carbonaceous materials, challenges in terms of cycle life, CE, and cell voltage remained. The strong Coulombic effect induced by trivalent Al cations made their electrochemical intercalation challenging, raising questions about the suitability of TMOs, particularly oxide anionic frameworks, as ideal hosts for RABs.
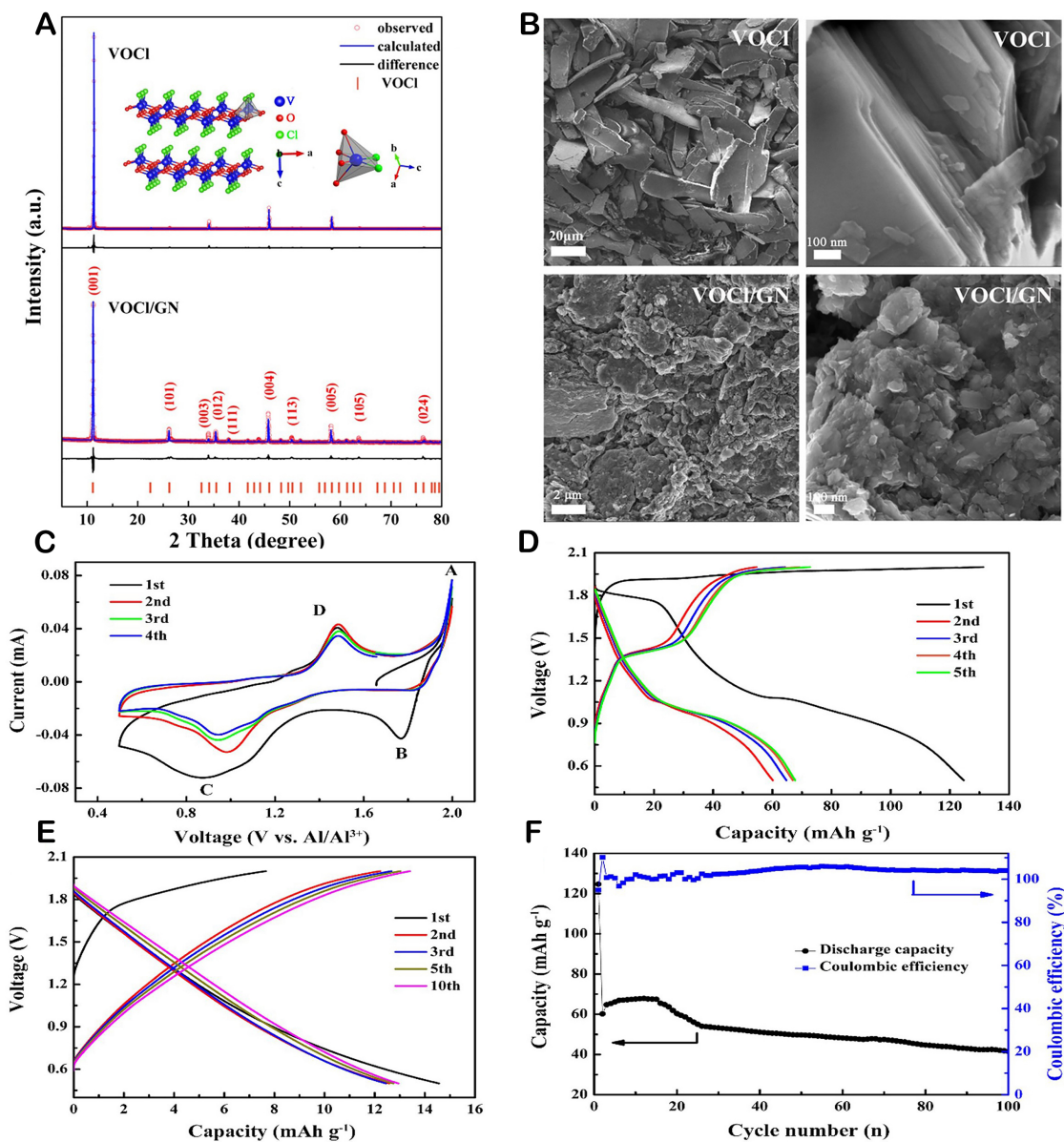
Figure 8. (A and B) XRD pattern and SEM images of VOCl and VOCl/GN, (C) cyclic voltammetry curves between 0.5- 2.0 V at a scan rate of 0.05 mVs^{-1}, (D) galvanostatic charge and discharge at a current density of 50 mAg^{-1}, (E) charge and discharge curves of GN electrodes at a current density of 50 mAg^{-1}, and (F) long-term cyclic performance at 50 mAg^{-1} of the VOCl/GN cathodes. Reproduced with permission ref.[151] copyright 2019 Elsevier.

MOF-based cathode materials

MOFs have garnered significant attention due to their impressive attributes, such as numerous micropores and a large specific surface area[154-156]. They are often combined with other substances to enhance the conductivity and stability of pure MOF-based materials, resulting in superior MOF-derived functional materials. These materials retain the porosity and surface area of original MOF crystals and may exhibit enhanced characteristics through synergistic interactions among functional units. Importantly, the structural properties of pristine MOFs are preserved under specific transformation conditions in the derived functional materials. In the literature, researchers have employed a straightforward hydrothermal method to synthesize MOF precursors, specifically HKUST-1[157-159]. Subsequent carbonization / tellurization treatment

yields CuTe@C composites with impressive features, including a high reversible capacity of 556.3 mAhg^{-1} and distinct charge/discharge voltage plateaus when used as the cathode in RABs. Another approach involves carbonization/tellurization via a single-step procedure to form the composite CoTe$_2$@N-PC. By combining zeolitic imidazolate framework (ZIF-67) nanocrystals and tellurium powder together, followed by pyrolyzing under an inert atmosphere, researchers have been able to obtain an improved rate capability of 635.8 mAhg^{-1} and a good cyclability of 168.6 mAhg^{-1} after 200 cycles[16]. The creation of a C@N-C@N, P-C graded heterojunction through precise tweaking of N, P doping in MOFs-derived porous carbon based on Zr-MOFs (UiO-66 and NH$_2$-UiO-66) and melamine phosphate (MPP) precursors. AIBs with these cathodes demonstrated superior capacity maintenance at high current densities.

To overcome the poor kinetics of graphite-based cathodes in RABs, Wang *et al.* reported a HCPO synthesized from the copper-based MOF[33], as shown in Figure 9A-C, and compared with graphite paper as a cathode, Al foil is used as an anode in IL electrolytes with anhydrous AlCl$_3$ and urea. This Al/Graphite battery was operated at room temperature and obtained a discharge capacity of 65 mAhg^{-1} over 150 cycles. The carbonaceous cathode possessed a unique hierarchical porous structure with high graphitic carbon in nature. It continued a specific capacity of 60.8 mAhg^{-1} after 200 cycles at 100 mAg^{-1}, along with a better rate performance than graphite cathode. However, despite showing good rate performance, still the capacity is low.

ELECTROLYTE REQUIREMENT

The choice of electrolyte plays a crucial role in the performance of batteries. An ideal electrolyte should facilitate the movement of ions between the electrodes, possess good conductivity, and ensure stability during the charging and discharging processes.

Non-aqueous electrolytes

Having composed of organic solvents, non-aqueous electrolytes offer a wider voltage window and are less prone to electrolysis, making them suitable for high-energy-density systems. They allow for the operation of batteries at higher voltages, contributing to increased energy density and overcoming the limitations of aqueous counterparts[148,160]. Moreover, non-aqueous electrolytes exhibit better stability at high voltages, reducing the risk of electrolyte decomposition and enhancing the overall performance and safety of the battery[136,161,162]. In summary, while aqueous electrolytes have advantages in terms of cost and conductivity, non-aqueous electrolytes offer a broader voltage window and improved stability, making them a preferred choice for specific high-performance and high-energy-density battery applications. The selection between aqueous and non-aqueous electrolytes depends on the specific requirements and constraints of the intended battery system.

In the pursuit of non-aqueous RABs, extensive research has focused on RTIL electrolytes for energy storage[163]. These have attracted attention due to their expansive potential windows and reduced vapor pressure. Nevertheless, despite their advantages, certain drawbacks warrant closer examination. Firstly, chloroaluminate-based ILs have increased prices and hygroscopic nature[61,62], limiting their widespread application on a large scale[164]. Secondly, challenges arise from unexpected side reactions occurring during energy storage, specifically the oxidation of AlCl$_4^-$ leading to the generation of Cl$_2$. This results in a comparatively lower CE and rapid capacity degradation in non-aqueous RABs. Additionally, the corrosive nature of chloroaluminate species significantly restricts choices for current collectors, necessitating the use of expensive and stable metals such as Mo and Ta.
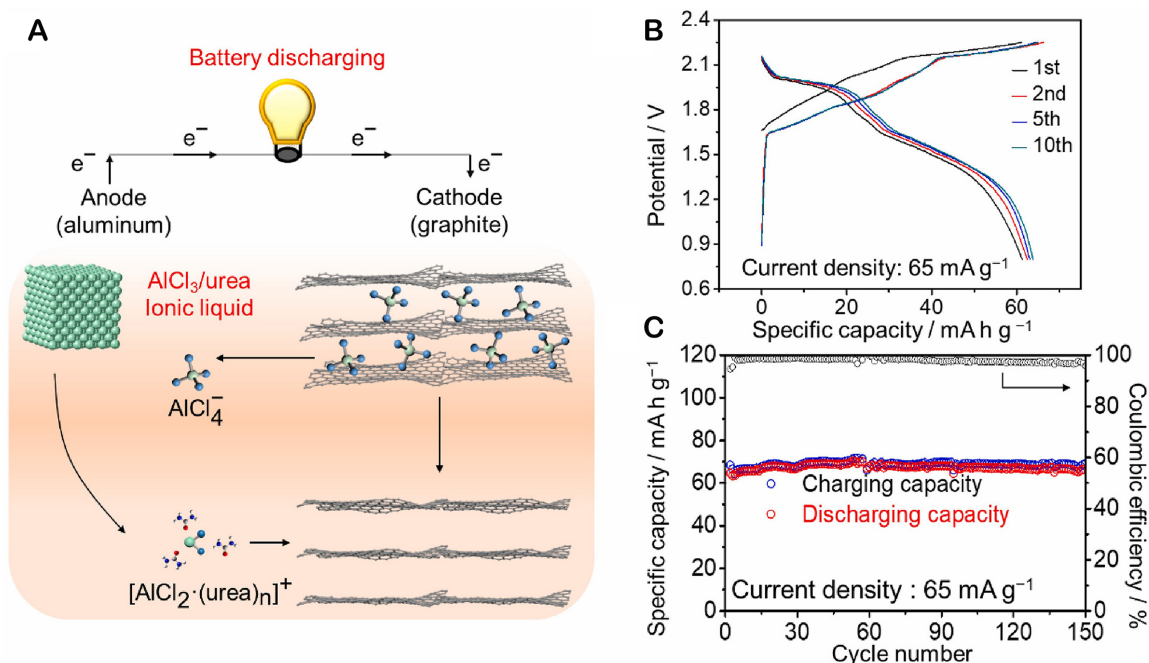
Figure 9. (A) Schematic of Al/graphite cell with $AlCl_3$ Urea-based ionic liquid electrolyte during discharge process at the anode side, metallic Al, $AlCl_4^-$ ions and urea formed at the cathode side, graphite has layered spaces, the $AlCl_4^-$ could intercalate and deintercalated during charge and discharge process, (B) charge/discharge curves, and (C) long-term stability of aluminum graphite battery at a current density of 65 mAg^{-1}. Reproduced with permission ref.[33] copyrights 2023 Elsevier.

The corrosive nature of IL electrolytes imposes an urged requirement for the development of cell prototypes. In contrast to LIBs or SIBs, non-aqueous RABs encounter limitations in using coin cells due to potential corrosion of the stainless-steel cap by chloroaluminate-based ILs. The corrosion is evident in the redox peaks in CV curves during cycling, attributed to the redox reaction among Fe and Cr with $Al_2Cl_7^-$. Numerous anticorrosive precautions have become necessary, including plating the electrodes with gold or capping them with titanium foil. Consequently, for practicality, pouch or Swagelok-type cells are commonly employed for measurements, as they can encapsulate the battery without relying on stainless steel and complex processes. Furthermore, the incompatibility of polymer binders such as PVDF with chloroaluminate-based ILs has been confirmed. As a result, there is a shift towards exploring more stable, cost-effective, and efficient electrolytes for RABs. Recent efforts include investigating IL-based electrolytes, GPEs, inorganic molten salt electrolytes, and organic IL electrolytes. This section provides an overview of current research trends, highlighting the improvements and drawbacks of non-aqueous RAB electrolytes.

Inorganic molten salts
Since the 1970s, significant progress has been made in aluminum batteries utilizing molten salts as electrolytes[165]. In one instance, a secondary Al-FeS$_2$ cell was developed using a molten $AlCl_3$/NaCl electrolyte, revealing discharge plateaus at approximately 0.6 and 0.9 V within a temperature range of 180-300 °C. Exploring electrolyte additives, the study found that $SnCl_2$ notably influenced cell performance. The same research group investigated the electrochemical behavior of FeS in molten $AlCl_3$/NaCl saturated with NaCl containing dissolved Al_2S_3, revealing oxidation reactions controlled by sulfide ion diffusion. Subsequent studies by[166] showed that incorporating N-1-butylpyridinium chloride (BPC) into $AlCl_3$/NaCl or $AlCl_3$/LiCl melts will decrease the operating temperature of Al-FeS$_2$ batteries to around 100 °C[23,167]. However, the batteries exhibited low cycling efficiencies during recharge at lower temperatures. Another approach involved using a low-melting electrolyte ($LiAlCl_4$/$NaAlCl_4$/$NaAlBr_4$/$KAlCl_4$) in a rechargeable

battery system with a Ni_3S_2 cathode at 100 °C. Early battery systems faced challenges in achieving high capacity and long cyclic life, attributed to the instability of active species in molten salts and the formation of aluminum dendrites. In 2017, a novel Al-graphite battery operating in an $AlCl_3$/NaCl melt electrolyte (molar ratio of 1:1.63) at 120 °C demonstrated impressive discharge capacities, cyclic stability over 9,000 cycles, and high coulombic efficiency.

Furthermore, the study explored the impact of operating temperature and $AlCl_3$ concentration in the electrolyte system, revealing optimal performance under an $AlCl_3$/NaCl molar ratio of 1:1.8 at 130 °C. The energy storage mechanism involved the intercalation/deintercalation of $AlCl_4^-$ and $Al_2Cl_7^-$ into/from graphitic layers[165]. Recent advancements include developing a ternary $AlCl_3$/LiCl/KCl molten salt system, delivering comparable performance at 99 °C to the $AlCl_3$/NaCl system at ≥ 120 °C. Additionally, a quaternary $AlCl_3$/NaCl/LiCl/KCl inorganic molten salt electrolyte exhibited excellent electrochemical and cycling performance at a remarkably low temperature of 75-90 °C. These findings highlight the promising application potential of inorganic molten salts as electrolytes for secondary aluminum batteries, particularly for grid-scale renewable energy storage, benefiting from their inherent low cost, low flammability, and outstanding performance metrics[166,167].

Organic ionic liquids
RTIL electrolytes have been extensively studied for RABs due to their operation at room temperature and numerous advantages, including low vapor pressure, non-flammability, and high electrical conductivity. In the mid-1980s, the first ambient temperature secondary aluminum batteries were established, utilizing electrolyte systems such as $AlCl_3$ and EMIC. Subsequent studies explored diverse organic IL systems, revealing the influence of halogen ions on electrochemical stability and conductivity. Notably, Et_3NHCl-based IL resulted in stable[143] Al-graphite batteries with enhanced performance and ultra-long cycling stability. Considering the high cost of certain ILs, alternative formulations such as $AlCl_3$/urea electrolytes were investigated, demonstrating reversible aluminum deposition/dissolution, and achieving high energy density. Additionally, eutectic $AlCl_3$/acetamide ILs and innovative organic electrolytes, such as $AlCl_3$/ imidazole hydrochloride and $AlCl_3$/caprolactam, were proposed, showing promising results in achieving high-rate capability and long-term cyclability. However, the highly reactive nature of $Al_2Cl_7^-$ species in organic IL electrolytes posed challenges to stability. To address this, non-corrosive alternatives such as aluminum trifluoromethanesulfonate $[Al(OTF)_3]$-based electrolytes were explored, showcasing favorable properties such as high ionic conductivity and an extended electrochemical window[168]. Despite the current performance gap compared to $AlCl_3$-based systems, these non-corrosive electrolytes present a new method for aluminum battery electrolyte development. Moreover, ILs based on the neutral complexation $AlCl_3$/4-ethyl pyridine ligands exhibited high reversibility in Al electrodeposition/stripping, showcasing promise for RAB applications with lower corrosivity compared to traditional systems.

Ionic liquid-based electrolytes
For LIBs, organic solvent-based electrolytes are commonly used; however, this approach is unsuitable for AIB systems[45]. As the aluminum ion contains three positive charges and high surface charge density, the Coulombic interaction between positive and negative ions is intensified reducing the solubility of aluminum ion salt in organic solvents. Ether solvents can enhance solubility through ion-dipole interactions but may lead to high electrodeposition polarization due to desolation activation energy. Fluorine-containing aluminum salts in organic solvents can form a passive layer on the aluminum anode, hindering reversible electro-stripping/deposition. Different anions in an IL electrolyte can lead to distinct anode-limiting potentials, influencing various corresponding anodic limiting reactions.

$$4AlCl_4^- - 2e^- \rightarrow Cl_2 + 2Al_2Cl_7^- \tag{16}$$

$$6Al_2Cl_7^- - 2e^- \rightarrow Cl_2 + 4Al_3Cl_{10}^- \tag{17}$$

$$2Cl^- - 2e^- \rightarrow Cl_2 \tag{18}$$

Which depict oxidation reactions associated with molar ratios equal to, higher than, or less than 1:1. Concerning cathode limiting reactions, a pair of redox peaks indicative of reversible aluminum stripping/ deposition is observed around 0 V when the molar ratio exceeds 1.5:1, emphasizing the significance of the $Al_2Cl_7^-$ anion[145]. The ionic conductivities of $AlCl_3$/EMIC IL electrolytes at different molar ratios are examined; aqueous electrolytes were initially applied in aluminum battery systems but faced drawbacks such as passive oxide film formation and hydrogen side reactions. High-temperature molten salts were later used, but they presented challenges such as extreme conditions and cathode disintegration. ILs emerged as a promising alternative, offering high electrochemical stability and favorable properties for energy storage. The IL-based electrolyte enables highly reversible stripping/plating of aluminum, making AIBs increasingly competitive in secondary batteries. ILs usually contain long-chain organic cations, such as imidazolium or pyrrolidinium, paired with anions such as Cl^-.

Gel electrolyte

Electrolyte leakage and unstable internal interfaces resulting from mechanical deformation, coupled with suboptimal porous textile separators, remain significant challenges in liquid electrolytes, particularly those utilizing glass microfiber membranes. To address these issues in liquid AIB systems, Kim *et al.* developed a flexible quasi-solid-state RAB featuring a GPE positioned between a graphite-based cathode and an Al-based anode[169]. Polyacrylamide served as a polymeric framework, providing mechanical and electrical insulating properties, while $AlCl_3$/EMIC ILs functioned as plasticizers for ionic conductors within the GPE. This quasi-solid-state RAB demonstrated superior performance to liquid systems, achieving an impressive specific capacity of 120 mAhg^{-1} at a current density of 60 mAg^{-1}. In another innovative approach, GPEs were created through *in-situ* polymerization of ethyl acrylates (EA) within $AlCl_3$/EMIC ILs. Poly-EA, with a glass transition temperature of approximately 24 °C, exhibited rubber-like flexibility at room temperature, making it suitable for use as a solid electrolyte in flexible batteries. The entire cell employing GPEs demonstrated superior cycle stability, high current density, and efficient ion transport compared to previous studies. Even at a high current density of 200 mAg^{-1}, it maintained an average discharge-specific capacity of 85 mAhg^{-1} and cycle retention of approximately 95% up to 500 cycles. Moreover, Liu *et al.* and Yu *et al.* introduced a distinctive GPE by blending PA with the low-cost $AlCl_3$/Et_3NHCl IL using a straightforward process[46,48]. After cooling, a PA-based GPE was generated by swirling and boiling PA into the acidic $AlCl_3$/ Et_3NHCl IL. The PA-based GPE exhibited a solid-like condition, demonstrating reduced sensitivity to moisture and leaky corrosion. RABs utilizing GPE and quasi-solid-state Al/graphite batteries showcased remarkable rate capability and cyclability. Furthermore, deep eutectic solvents, resulting from the combination of a strong Lewis acidic metal halide and a Lewis primary ligand [e.g., $AlCl_3$/acetamide (AcA)-1.3], emerged as cost-effective ILs that demonstrated higher specific capacity with comparable physical and electrochemical properties. Another study utilized free radical polymerization for the first time to create a GPE incorporating $AlCl_3$-complexed acrylamide as a vital monomer and an acidic IL based on a mixture of EMIC and $AlCl_3$ (EMIC-$AlCl_3$, 1:1.5 in molar) as a plasticizer. This innovative RAB system holds promise for enhanced performance and stability. To explore the electrochemical energy storage mechanism in Aluminum graphite batteries with GPEs, as demonstrated in Figure 10A and B, *in situ* X-ray diffraction (XRD) and operando Raman spectroscopy are performed during the charging and discharging processes at a constant current density. Initially, the pristine graphite exhibits a prominent (002) peak at $2\theta = 26.5°$
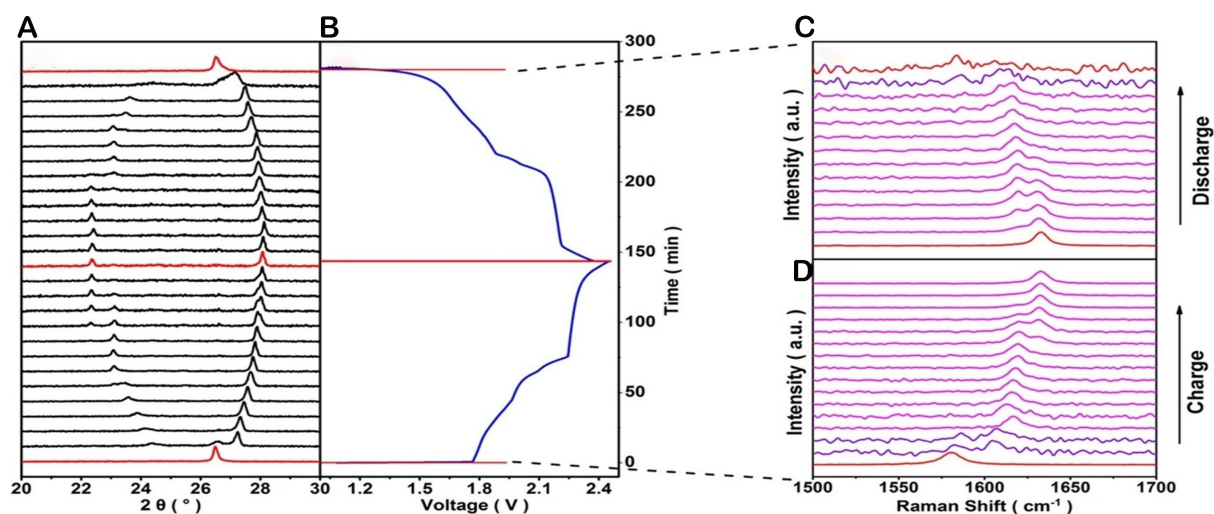
Figure 10. (A) XRD spectrum of the graphite cathode in the Al/GPE/graphite battery during charge-discharge process origin, (B) corresponding charge-discharge profile Al/GPE/graphite battery, operando Raman spectra on the graphite cathode (C) discharging, and (D) charging processes. Reproduced with permission ref.[46] Copyrights 2021 American Chemical Society.

corresponding to a d-spacing of 3.36 Å. As charging progresses, the (002) peak gradually fades, and two new peaks emerge on either side of the original (002) peak. This change signifies the formation of a graphite-intercalated compound (GIC) due to anion intercalation into the graphite layers. The charge-discharge profiles for this process are illustrated in Figure 10C and D. At full charge, the graphite reaches stage 3. The operando Raman spectra of the graphite cathode during charging and discharging reveal that, during charging, the G-band (1,582 cm^{-1}) splits into two Raman modes: a lower-frequency component E_{2g2i} (1,586 cm^{-1}) and a higher-frequency component E_{2g2b} (1,609 cm^{-1}). These modes are attributed to the vibrations of carbon atoms in non-intercalated and intercalated graphite layers, respectively.

ANALYSIS OF MICROSTRUCTURE IN RABS

The exploration of the microstructure's impact on electrodes in non-aqueous RABs seeks to uncover intricate aspects of battery chemistry investigating interactions with the electrolyte, corrosion studies, and the plating/stripping process. The quest for suitable anodes for non-aqueous RABs beyond aluminum remains an ongoing endeavor[120,162]. Researchers persist in unraveling the effects of the chemical nature and geometries of various materials, including Al foil, graphite, and stainless steel, that influence the reversibility of the reaction and the overall performance of the battery. As depicted in Figure 11A-C, observations reveal that in aluminum's stripping and plating process, the reactions involving Al foil and expanded graphite demonstrated reversibility, whereas those involving stainless steel did not. Prolonged reduction under negative current density revealed uniform and compact coverage of Al deposits on the surfaces of Al foil and expanded graphite, contrasting with poorly adhered and heterogeneous deposits observed on stainless steel. Furthermore, an extended electroplating period led to an increase in CE from 80% to 100%, as illustrated in Figure 11D-I. These findings suggest that, apart from aluminum, expanded graphite emerges as a promising candidate for aluminum batteries as an anode. A comparison between flat expanded graphite and 3D carbon paper demonstrated higher Coulombic efficiencies and lower overpotentials for the plating/stripping reaction[162] with the latter, suggesting that 3D architectures provide advantages for anodes. This principle applies to other electrodes, such as Al mesh, affirming the potential for achieving higher power densities with 3D-structured anodes. Simultaneously, cost-effective and corrosion-resistant Al alloys have been utilized as anodes in RABs to address economic considerations.
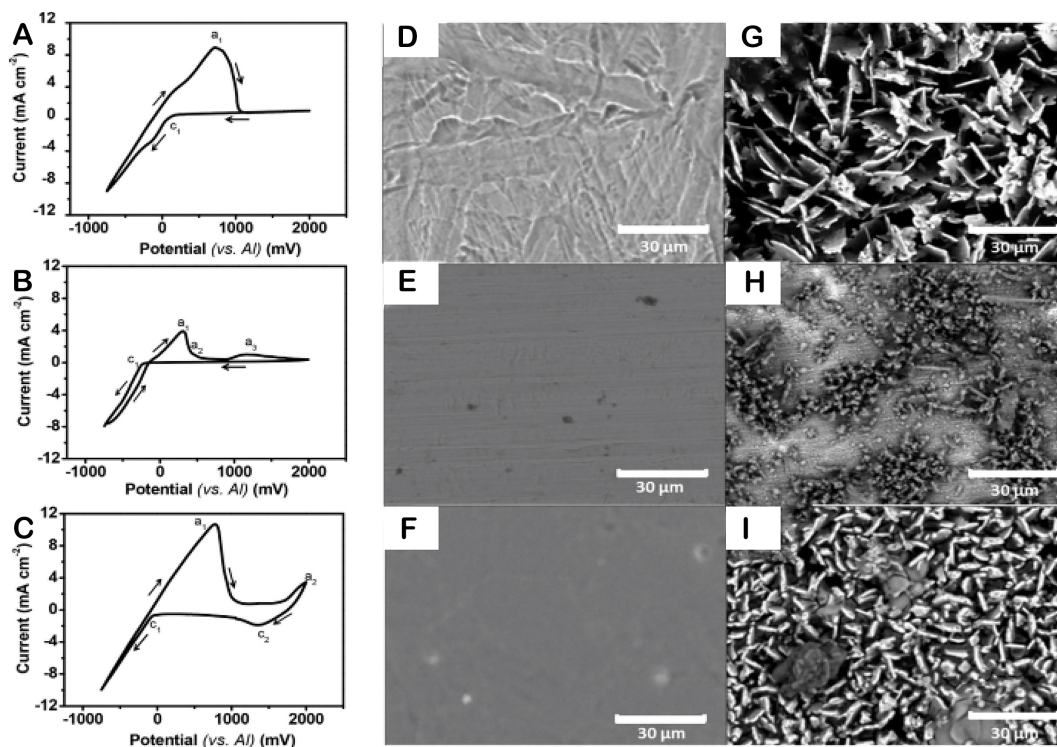
Figure 11. Cyclic voltammetry of (A) aluminum foil, (B) stainless steel foil, and (C) expanded graphite in AlCl₃/EMIC SEM images of substrates before and after long Al electrodeposition, (D, G) Al foil, (E, H) stainless steel, and (F, I) expanded graphite. Reproduced with permission ref.[120] Copyrights 2018 Elsevier.

Aluminum alloy passivation films play a crucial role in hindering the deposition and dissolution of aluminum. The optimal condition for generating the battery is achieved at a temperature of 130 °C with an AlCl₃/urea ratio of 1.5 mole [Figure 12] to ensure Coulomb efficiency remains above 90%, the cut-off voltage for the aluminum alloy/Pyrolytic Graphite (PG) battery is set at 2.18 V, resulting in the highest observed efficiency [Figure 12A]. Lower efficiency, likely caused by side reactions, significantly beyond 2.18 V, is noted in the electrolyte. Current density serves as a reflection of the electrochemical reaction rate[162]. At lower currents, active material utilization is more comprehensive, while higher currents lead to increased electrode polarization, potentially limiting active material utilization. Across various current densities of 100, 150, and 200 mAg⁻¹, the aluminum alloy/PG battery maintains approximately 90% ± 5% coulombic efficiency over 30 cycles [Figure 12B]. Initial coulombic efficiency exceeding 100% is attributed to incomplete electrolyte saturation in the early cycles, preventing complete battery charging. The specific capacity starts at 105 mAhg⁻¹ at a current density of 100 mAg⁻¹ [Figure 12C and D], gradually decreases, and stabilizes at 94 mAhg⁻¹, displaying notable capacity performance. Capacitance attenuation may result from electrolyte evaporation and pyrolytic graphite instability. Overall, the aluminum alloy initially flat undergoes partial corrosion after 80 cycles yet remains smooth without dendritic aluminum formation. Notably, the aluminum alloy exhibits better corrosion resistance and cost-effectiveness than pure Al foil, as confirmed by SEM and energy dispersive X-ray spectroscopy (EDS) images before cycling and after 80 cycles, showing minimal changes in the alloy surface composition. Figure 12E and F presents the thermal studies at 100-130 °C of charge-discharge curves, where the voltage range is from 0.4 to 2.18 V, with the average charge-discharge voltages being around 1.9 and 1.6 V, respectively. The electrolyte mole ratio of 1.5 mole shows a higher capacity than 1.4 mole electrolytes with the same temperature. Figure 12G and H indicates that the CV curves of the aluminum alloy anode and PG cathode in the electrolyte AlCl₃/urea of 1.5 and 1.4 mole show better yield having good electrochemical performance. It is interesting to observe as the temperature rises, the capacity also increases.
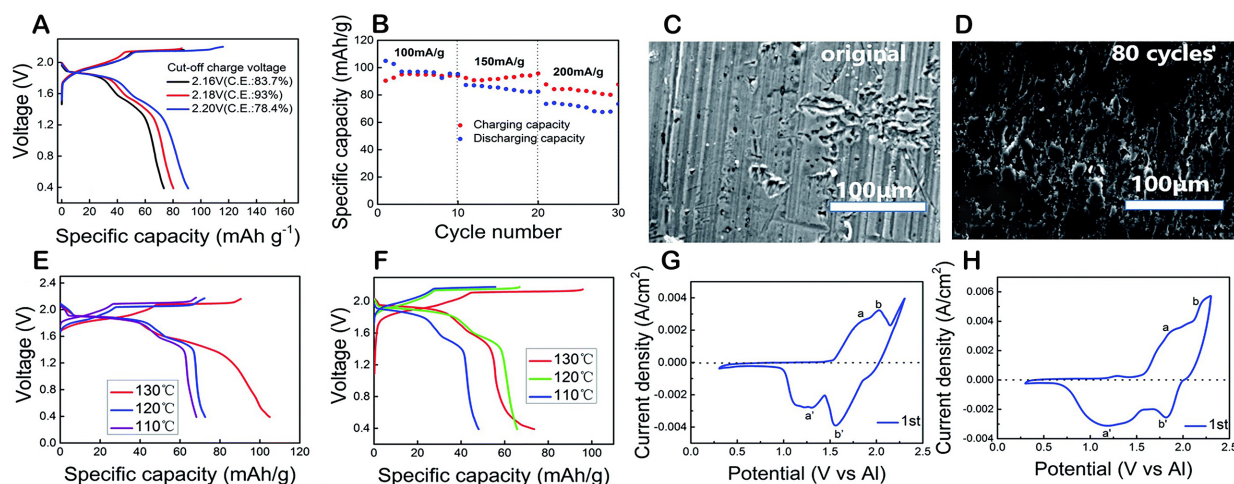
Figure 12. (A) Galvano static curves of aluminum alloy/PG cells with different cut-off charge voltages at 100 mAg^{-1}, (B) An aluminum alloy/PG cell is charging and discharging with a current density from 100 to 200 mAg^{-1}, (C) SEM images of the original Al alloy anode obtained from aluminum alloy/PG cells, (D) After 80 cycles respectively indicate no dendrite formation, (E) charge-discharge cycles with different temperatures in an AlCl$_3$/urea of 1.5 mole at 100 mAg^{-1}, (F) charge-discharge cycles with different temperatures in a 1.4 mole AlCl$_3$/urea electrolyte, and (G and H) cyclic voltammetry studies in AlCl$_3$/urea of 1.5 & 1.4-mole liquid electrolyte. Reproduced with permission ref.[162] Copyrights Royal Society of Chemistry.

The aluminum anode displays chemical instability in the IL electrolyte due to the corrosive nature of Lewis acidic chloroaluminate anions[11]. The chemical activity and stability of aluminum in ILs were investigated by monitoring morphological changes on the aluminum surface. Results revealed the localized dissolution of the pristine oxide layer and the formation of a new oxide layer, rather than aluminum ions Al^{3+} diffusing into the electrolyte[170,171]. The interface between the anode and electrolyte plays a pivotal role in the performance of non-aqueous RABs. Challenges related to the interface encompass electrochemical reactions, composition, and structure of interfacial layers, ion transport, and kinetic behavior. A comprehensive understanding of interface formation is crucial for developing high-performance, non-aqueous aluminum batteries. Figure 13 illustrates the design of the anode/electrolyte interface for non-aqueous aluminum batteries. Interface regulation can be achieved through alloying, grain refinement, surface modification of aluminum anodes, and the incorporation of electrolyte additives. Moreover, successful strategies for the interface regulation of lithium and zinc anodes can be adapted for aluminum anodes. Consequently, controlling electron and ion transfer at the interface through interfacial regulation enables improved stripping/plating behavior of the aluminum anode, contributing to enhanced performance in aluminum-based batteries. These modifications to the anode and the design strategies for interfacial control are anticipated to be effectively applied, leading to high-performance RABs.

ADVANCED TECHNOLOGIES FOR CHARACTERIZATION

Due to their dynamic, real-time, and intuitive nature, researchers prefer employing *in situ* characterization techniques for the study of secondary batteries[58,59]. These techniques enable the exploration of morphology and structure evolution, as well as the redox reaction processes of battery materials. Despite significant progress in applying various characterization techniques to non-aqueous RABs, several fundamental scientific issues remain to be comprehensively investigated. These issues span from the material to electrode to battery levels, encompassing nanoscale, microscale, and macroscale dimensions.
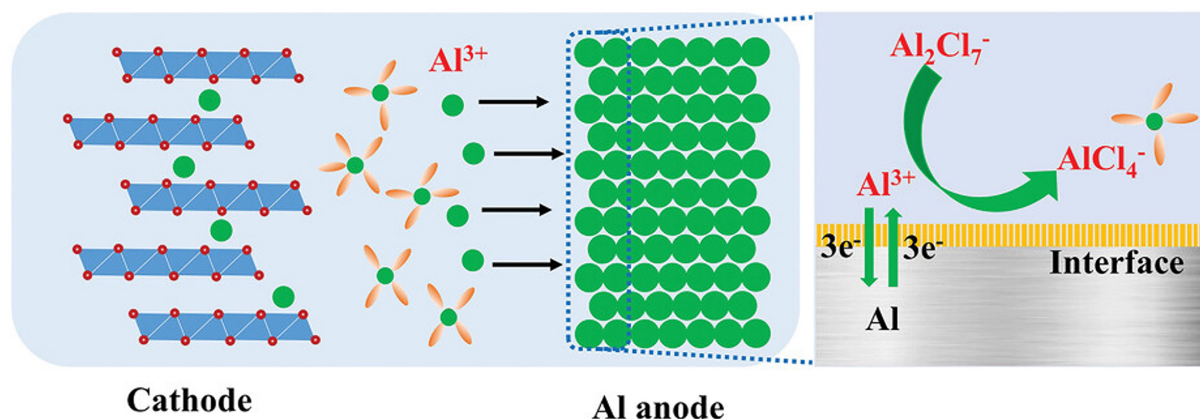
Figure 13. The design of anode/electrolyte interface of a non-aqueous AIB. Reproduced with permission ref.[11] Copyrights 2021 Wiley-VCH.

Because of the side reactions triggered by the strong acidity of IL electrolytes, most electrode materials reported in non-aqueous RAB studies utilize *ex-situ* techniques[1]. *In situ* XRD, transmission electron microscopy (TEM), SEM, and Raman characterizations predominantly concentrate on graphite cathodes. Real-time monitoring of physical and chemical transformations during discharge and charge processes, along with understanding thermal characteristics and behaviors in operando states, underscores the essential need for designing *in situ* cells. Particularly in acidic electrolytes with non-graphite electrode materials, there is an urgent need for various *in situ* analytical methods, including *in situ* XRD, Raman, X-ray photoelectron spectroscopy (XPS), SEM, TEM, atomic force microscopy (AFM), infrared spectra, stress tests, and, to identify ionic diffusion and reaction processes, thermal and mechanical behaviors, interfacial phenomena, chemical stability of electrodes, evolution, structural, and infrared thermal imaging in non-aqueous RABs.

Addressing these challenges requires a multiscale approach, combining various techniques such as *in situ* and *ex-situ* to provide valuable insights. For instance, understanding the electro-chemo-mechanical coupling mechanisms during the intercalation/deintercalation of Al complex ions in active materials can benefit from real-time strain measurements and observations of ionic transport and diffusion processes. However, achieving further advancements in this field requires continued efforts and exploration.

CHALLENGES OF NON-AQUEOUS RABS

Non-aqueous RABs have gained attention as potential energy storage devices, but they also face several challenges that need to be addressed for widespread adoption. RABs, whether in primary or secondary systems, encounter various scientific and technological challenges that hinder their practical applications. One such challenge arises from the naturally formed alumina layer on the aluminum anodes, impacting their electrochemical behavior. The formation of Al dendrites further presents a significant issue that adversely affects the energy density and safety of RABs. Additionally, the cycling performance of some aluminum batteries faces constraints due to volume expansion resulting from alloying/de-alloying reactions. Despite the promising application prospects and recent notable advancements in non-aqueous RABs, they still grapple with significant challenges related to inadequate reaction kinetics, low energy density, and pronounced capacity fading. These challenges primarily revolve around five key aspects: cathodes and anodes, electrolytes, current collectors, and binders. *Cathode materials:* Developing highly efficient cathode materials for RABs is a challenge. Finding materials capable of reversibly intercalating Al ions while providing both high capacity and stability remains a significant hurdle. *Anode materials:* The development

of suitable anode materials is crucial. Al can form a passivation layer that hinders ion transport, leading to poor electrode kinetics. Overcoming this passivation layer is a key challenge. *Aluminum plating/stripping*: During the charging and discharging process, aluminum can plate onto the anode and strip during discharge. However, controlling aluminum deposition and dissolution can be challenging, leading to dendrite formation and safety concerns. *Cycle life*: Ensuring a long cycle life with minimal capacity degradation over repeated charge-discharge cycles is a persistent challenge. Electrode materials and electrolyte stability are crucial in achieving a prolonged cycle life. *Scale-up and manufacturing*: Transitioning from lab-scale prototypes to large-scale manufacturing can be challenging. Developing scalable processes and maintaining consistent quality control are essential for mass production. *Environmental Impact*: The environmental impact of the materials used in RABs and the recycling processes should be considered. Sustainable and environmentally friendly practices are increasingly important in developing energy storage technologies. The two significant challenges are discussed below.

Passivation/dendrite formation

Al has been extensively utilized in traditional battery configurations due to its numerous advantages. Yet, several inherent challenges persist, including: (1) the formation of a surface passivation layer on the Al electrode, resulting in reduced battery voltage and performance; (2) serious corrosion resulting in irreversible utilization of aluminum and diminished further availability of the Al for subsequent reaction; and (3) dendrite formation during cycling compromising battery safety and cycle life. The passivation film, primarily Al_2O_3, on the Al metal is known for its role as a highly effective electrical/ionic insulator, interfering with the redox reactions on the electrode surface. This Al_2O_3 layer also decreases electrochemical activity, protecting Al metal against severe dissolving tendency in acidic electrolytes. Numerous reports have affirmed the impact of the oxide film on the dissolution and dendrite formation on the Al electrode. For instance[160,162], investigated and compared the surface morphology of electro-polished and native Al immersed in acidic $AlCl_3$/EMIC IL electrolyte for a range of duration. The electro-polished Al initially exhibited a pure, smooth Al surface[170]. However, after prolonged soaking, surface damage, such as cracks and pits, became more apparent. The native Al displayed a somewhat rugged and rough surface due to the presence of the native oxide film. With increased linear cracks, immersion times, and a distorted surface were observed, albeit with minimal fracture. Similar observations were made when the oxide film on the Al metal surface was aggressively cracked by acidic $AlCl_3$/BMIC IL. This suggests that while the oxide film can partially suppress the dissolution of bulk Al, the Al foil remains susceptible to attack chloride complexes in acidic electrolytes, irrespective of the oxide film on the Al surface also noted severe corrosion on the Al surface with increasing dipping time. Furthermore, a higher concentration of $Al_2Cl_7^-$ anions resulted in more pronounced corrosion, indicating elevated electrochemical activity. Notably, the Al surface dissolved along a specific lattice plane, and deeper cracks formed as the acidic electrolyte penetrated the cracking sites to react with internal Al metal at the metal/oxide interface. Particularly noteworthy was the observation that newly formed Al oxide accumulated around the cracking sites, indicative of localized attack by chloroaluminate anions, leading to the creation of a new Al_2O_3 oxide layer on specific lattice planes.

However, researchers tend to believe that the aluminum oxide on the Al surface should be eliminated to enhance electrochemical activity. Pre-immersion in chloroaluminate IL can activate the aluminum anode by partially removing the aluminum oxide layer. Moderate removal of oxide layers renders the Al surface more reactive to the electrolyte. The removal of the oxide film has been shown to increase the coulombic efficiency of aluminum dissolution/deposition, while excessive removal does not show improvement. These results indicate the anti-corrosion nature of the aluminum anode. The native aluminum growth can suppress dendrite formation to stabilize the electrolyte/anode interface. In conclusion, the presence of surface aluminum oxide can passivate and stabilize the aluminum anode[49,172]. The traditional electrode kinetics suggest that LIBs primarily involve the migration of Li^+ cations between cathodes and anodes in a

rocking-chair fashion. In contrast, RABs, characterized by a dual-anion or dual-ion mechanism, engage $AlCl_4^-$ and $Al_2Cl_7^-$ anions or Al^{3+} cations and $Al_2Cl_7^-$ anions simultaneously. Consequently, these batteries exhibit distinct behaviors in mass transport, electrode transfer, and internal diffusion within solids. Due to the intricacies of processes in RABs, pinpointing the rate-determining step in electrode kinetics becomes challenging. The outcomes of thermodynamic and kinetic parameters in RABs are the crucial importance of comprehending electrode kinetics in the electrochemical process. Clearly, substantial attention should be devoted to experimentally assessing various parameters, encompassing transport and diffusion processes in the bulk electrolyte and electrode. This includes considerations of binding energy, electrode potential, exchange current density, diffusion coefficient, ionic migration time, and related factors. Consequently, a thorough analysis of thermodynamics and kinetics in RABs is pivotal for guiding the design of electrolytes with a broader electrochemical window and enhanced conductivity. Additionally, it plays a vital role in optimizing electrode materials by seeking those with higher potential, smaller migration distances, and increased diffusion paths[1].

Obstacles of non-aqueous electrolytes

Non-aqueous electrolytes can be prone to decomposition and instability over repeated charge-discharge cycles. This can lead to the formation of unwanted by-products, affecting the battery's performance and lifespan. In non-aqueous electrolytes, apart from the significant cost implications, several critical issues exist. For example, (1) Limited electrochemical window: The narrow electrochemical window presents challenges, resulting in reactions such as electrolyte decomposition and undesirable gas evolution. This limitation prevents cathodes from charging to higher voltages, leading to reduced energy density; (2) Serious corrosion effects: The non-aqueous environment exacerbates corrosion, causing the degradation and dissolution of both binders, current collectors, and electrodes; (3) Anion species characteristics: The wide radius of anion species necessitates strong structural stability for intercalation-type positive materials. However, this characteristic also contributes to low ionic movement and charge transfer rates. In Al-Se batteries, the pristine long se nanowires undergo shortening and even disappearance during charging, a state upon full discharge. This phenomenon primarily arises from the dissolution of the charged product Se_2Cl_2 in the acidic electrolyte. This process leads to a decrease in active material, and unregulated interfacial deposition results in a decline in chloroaluminate anion transport. These effects cause voltage and capacity degradation; and (4) Weak electrolyte-electrode interface: The electrolyte-electrode interface faces challenges in terms of weak interaction, leading to high interfacial resistance and hindered ionic and electronic movement. This interface involves both the anode-electrolyte interface and the cathode-electrolyte interface. Within this context, the utilization of RTIL in Al-graphite batteries introduces instability in the cathode-electrolyte interface due to mechanical deformation[165,172].

Addressing these challenges requires collaborative efforts from researchers, engineers, and industry stakeholders. Continuous advancements in materials science, electrochemistry, and battery engineering are essential for overcoming these hurdles and making non-aqueous RABs a viable and competitive energy storage solution.

CONCLUSION AND FUTURE POTENTIAL

RABs present the combination of electrode material stability, enhanced ion mobility, formation of passivation layers, lower electrochemical potential, and reduced dendrite formation collectively contributing to their fascinating substitutes to presently available commercial batteries in energy storage systems, showcasing significant potential due to their attributes such as cost effectiveness, high capacity, long cyclability, safety in use and chemical composition range. A comprehensive comparison is conducted between RABs and three other commercially used LIBs, battery systems - lead-acid batteries and nickel-

metal hydride (Ni-MH) batteries to discern the disparities between laboratory development and commercialization. Each battery system exhibits distinct advantages and disadvantages, with none encompassing all highly efficient features simultaneously. While cost-effective and safe, lead-acid batteries grapple with issues of low energy density and short cycle life. LIBs, renowned for their high energy density, encounter challenges tied to inherent security concerns, limited cycle life, and the scarcity of lithium resources, hindering their further development. Moreover, these current battery systems exhibit compromised electrochemical performance, particularly at extreme temperatures, where safety concerns escalate, significantly beyond 70 °C. Despite current limitations in energy density and higher costs, RABs offer significant advantages such as prolonged cycle life, superior wide-temperature performance, and excellent safety. These attributes position RABs favorably for large-scale commercialization. While reported cathode energy densities in RABs remain below 200 Whkg^{-1}, their overall benefits make them promising candidates for practical applications, especially considering the comprehensive performance they offer. Structural configurations play a pivotal role in scaling up practical cells, and the review scrutinizes the pros and cons of integrating well-established structural configurations from LIBs into RABs. Six key parameters are considered for evaluation, including flexibility in capacity, mechanical stress for electrode deformation, cyclability, package efficiency, battery performance firmness, and cooling efficiency. The review underscores the necessity for collaborative efforts to transition from lab-scale pouch cells to practical Ah-scale cells with carefully adjusted configurations. Despite recent progress in RABs, challenges persist across various electrode materials, including issues related to low capacity, substantial expansion in volume during intercalation reactions, poor intrinsic conductivity, and severe dissolution. Addressing these challenges requires effective approaches such as design modifications, flexible electrodes, improved anodes, enhanced current collectors, optimized binders, electrolyte modifications, and hybrid system designs. Additionally, systematic investigations into the electrochemical mechanisms of anions in aluminum batteries are crucial for understanding reaction kinetics and capacity degradation mechanisms.

The future potentials of RABs are promising, offering several advantages that could contribute to the evolution of energy storage technologies. Some key future potential includes *High energy density*: Aluminum batteries have the potential for high energy density, which could lead to long-lasting and more powerful energy storage solutions compared to current technologies. *Low Cost:* Aluminum is abundant and relatively inexpensive, which could contribute to developing cost-effective battery systems. This affordability might make aluminum batteries more accessible for various applications. *Fast charging and discharging:* Aluminum batteries have demonstrated the capability for rapid charging and discharging, making them suitable for applications because the overall combination of low internal resistance, high ionic conductivity, and stable electrode-electrolyte interface where quick energy release is crucial, such as electric vehicles and portable electronic devices. *Safety:* Owing to the non-flammable nature of aluminum, these batteries have the potential to be safer compared to some lithium-ion counterparts. This could make them attractive for applications where safety is a critical concern. *Scalability:* Aluminum batteries have the potential to be scalable for various applications, from small electronic devices to large-scale grid storage. This scalability is crucial for accommodating the diverse energy storage needs of different industries. *Technology advancement:* Ongoing research and technological advancements are likely to address current challenges and optimize the performance of aluminum batteries, unlocking their full potential and expanding their range of applications. Aluminum batteries could play a key role in storing energy generated from renewable sources, contributing to the stability and reliability of renewable energy systems. This integration aligns with the global shift toward sustainable and clean energy solutions. As research and development efforts continue, RABs promise to become a competitive and environmentally friendly option in the rapidly evolving field of energy storage. Realizing these potentials will depend on overcoming current challenges and further optimizing the technology for widespread commercial use. In conclusion, passivation and bulging of electrodes are two main major disadvantages RABs face; further research has to continue mainly

to tackle the major problems; the bulging of electrodes can be controlled by the shot peening/shot blasting method. By the shot peening method, the tensile stress of the material can be converted into residual stress. For passivation, major research focuses on pure aluminum, with only a few studies investigating aluminum alloys. RABs hold immense promise for high-performance energy storage systems, and ongoing efforts to overcome challenges and explore innovative solutions are essential for widespread adoption. Future development should prioritize addressing bottlenecks in electrode materials, achieving high energy density, ensuring cost-effectiveness, and exhibiting ranged-temperature performance. The review aims to provide valuable visions into the potential growth of practical RABs, stressing the need for continued global collaboration and efforts in the field.

DECLARATIONS

Authors' contributions
Conceptualization, investigation, and writing-original draft: Thatipamula S
Writing-review & editing: Thatipamula S, Malaarachchi C, Alam MR
Writing-review & editing, supervision, and funding acquisition: Khan MW, Mahmood N, Babarao R

Availability of data and materials
Not applicable.

Financial support and sponsorship

Conflicts of interest
All authors declared that there are no conflicts of interest.

Ethical approval and consent to participate.
Not applicable.

Consent for publication
Not applicable.

Copyright

REFERENCES

1. Tu J, Song WL, Lei H, et al. Nonaqueous rechargeable aluminum batteries: progresses, challenges, and perspectives. *Chem Rev* 2021;121:4903-61. DOI
2. Yang H, Li H, Li J, et al. The rechargeable aluminum battery: opportunities and challenges. *Angew Chem Int Ed* 2019;58:11978-96. DOI
3. Das S, Manna SS, Pathak B. Recent trends in electrode and electrolyte design for aluminum batteries. *ACS Omega* 2021;6:1043-53. DOI PubMed PMC
4. Zhang Y, Liu S, Ji Y, Ma J, Yu H. Emerging nonaqueous aluminum-ion batteries: challenges, status, and perspectives. *Adv Mater* 2018;30:e1706310. DOI
5. Jayaprakash N, Das SK, Archer LA. The rechargeable aluminum-ion battery. *Chem Commun* 2011;47:12610-2. DOI PubMed
6. Abu Nayem SM, Ahmad A, Shaheen Shah S, Saeed Alzahrani A, Saleh Ahammad AJ, Aziz MA. High performance and long-cycle life rechargeable aluminum ion battery: recent progress, perspectives and challenges. *Chem Rec* 2022;22:e202200181. DOI PubMed
7. Li Q, Bjerrum NJ. Aluminum as anode for energy storage and conversion: a review. *J Power Sources* 2002;110:1-10. DOI
8. Ferdian D, Pratesa Y, Togina I, Adelia I. Development of Al-Zn-Cu alloy for low voltage aluminum sacrificial anode. *Procedia Eng* 2017;184:418-22. DOI
9. Ran Q, Zeng S, Zhu M, et al. Uniformly MXene-grafted eutectic aluminum-cerium alloys as flexible and reversible anode materials

for rechargeable aluminum-ion battery. *Adv Funct Mater* 2023;33:2211271. DOI

10.   Wang M, Zhang F, Lee C, Tang Y. Low-cost metallic anode materials for high performance rechargeable batteries. *Adv Energy Mater* 2017;7:1700536. DOI

11.   Jiang M, Fu C, Meng P, et al. Challenges and strategies of low-cost aluminum anodes for high-performance Al-based batteries. *Adv Mater* 2022;34:e2102026. DOI

12.   Mahmood A, Ali Z, Tabassum H, et al. Carbon fibers embedded with iron selenide (Fe_3Se_4) as anode for high-performance sodium and potassium ion batteries. *Front Chem* 2020;8:408. DOI PubMed PMC

13.   Jiang J, Li Y, Liu J, Huang X, Yuan C, Lou XW. Recent advances in metal oxide-based electrode architecture design for electrochemical energy storage. *Adv Mater* 2012;24:5166-80. DOI

14.   Zafar ZA, Imtiaz S, Razaq R, et al. Cathode materials for rechargeable aluminum batteries: current status and progress. *J Mater Chem A* 2017;5:5646-60. DOI

15.   Wang DY, Wei CY, Lin MC, et al. Advanced rechargeable aluminium ion battery with a high-quality natural graphite cathode. *Nat Commun* 2017;8:14283. DOI PubMed PMC

16.   Tu J, Wang W, Lei H, Wang M, Chang C, Jiao S. Design strategies of high-performance positive materials for nonaqueous rechargeable aluminum batteries: from crystal control to battery configuration. *Small* 2022;18:e2201362. DOI

17.   Li Q, Mahmood N, Zhu J, Hou Y, Sun S. Graphene and its composites with nanoparticles for electrochemical energy applications. *Nano Today* 2014;9:668-83. DOI

18.   Mahmood N, Tang T, Hou Y. Nanostructured anode materials for lithium ion batteries: progress, challenge and perspective. *Adv Energy Mater* 2016;6:1600374. DOI

19.   Angell M, Pan CJ, Rong Y, et al. High coulombic efficiency aluminum-ion battery using an $AlCl_3$-urea ionic liquid analog electrolyte. *Proc Natl Acad Sci USA* 2017;114:834-9. DOI PubMed PMC

20.   Heise GW, Schumacher EA, Cahoon NC. A heavy duty chlorine-depolarized cell. *J Electrochem Soc* 1948;94:99. DOI

21.   Zaromb S. The use and behavior of aluminum anodes in alkaline primary batteries. *J Electrochem Soc* 1962;109:1125. DOI

22.   Egan D, Ponce de León C, Wood R, Jones R, Stokes K, Walsh F. Developments in electrode materials and electrolytes for aluminium - air batteries. *J Power Sources* 2013;236:293-310. DOI

23.   Gifford PR, Palmisano JB. An aluminum/chlorine rechargeable cell employing a room temperature molten salt electrolyte. *J Electrochem Soc* 1988;135:650-4. DOI

24.   Paranthaman MP, Brown G, Sun XG, Nanda J, Manthiram A, Manivannan A. A transformational, high energy density, secondary aluminum ion battery. *Meet Abstr* 2010;MA2010-02:314. DOI

25.   Sun H, Wang W, Yu Z, Yuan Y, Wang S, Jiao S. A new aluminium-ion battery with high voltage, high safety and low cost. *Chem Commun* 2015;51:11892-5. DOI

26.   Sun XG, Bi Z, Liu H, et al. A high performance hybrid battery based on aluminum anode and $LiFePO_4$ cathode. *Chem Commun* 2016;52:1713-6. DOI

27.   Zhang L, Zhang C, Ding Y, Ramirez-meyers K, Yu G. A low-cost and high-energy hybrid iron-aluminum liquid battery achieved by deep eutectic solvents. *Joule* 2017;1:623-33. DOI

28.   Tian H, Zhang S, Meng Z, He W, Han W. Rechargeable aluminum/iodine battery redox chemistry in ionic liquid electrolyte. *ACS Energy Lett* 2017;2:1170-6. DOI

29.   Wang S, Jiao S, Song W, et al. A novel dual-graphite aluminum-ion battery. *Energy Stor Mater* 2018;12:119-27. DOI

30.   Yu Z, Jiao S, Li S, et al. Flexible stable solid-state Al-ion batteries. *Adv Funct Mater* 2019;29:1806799. DOI

31.   Liu Y, Yang L, Xie B, et al. Ultrathin Co_3O_4 nanosheet clusters anchored on nitrogen doped carbon nanotubes/3D graphene as binder-free cathodes for Al-air battery. *Chem Eng J* 2020;381:122681. DOI

32.   Thanwisai P, Chaiyapo N, Phuenhinlad P, et al. Mesoporous and defective activated carbon cathode for $AlCl_4^-$ anion storage in non-aqueous aluminium-ion batteries. *Carbon* 2022;191:195-204. DOI

33.   Wang L, Zhu G, Lin Y, Wang Y, Zhu Q, Dai Z. MOF-derived hierarchical porous carbon octahedrons for aluminum-ion batteries. *Carbon* 2023;202:305-13. DOI

34.   Elia GA, Marquardt K, Hoeppner K, et al. An overview and future perspectives of aluminum batteries. *Adv Mater* 2016;28:7564-79. DOI

35.   Leisegang T, Meutzner F, Zschornak M, et al. The aluminum-ion battery: a sustainable and seminal concept? *Front Chem* 2019;7:268. DOI PubMed PMC

36.   Han X, Bai Y, Zhao R, Li Y, Wu F, Wu C. Electrolytes for rechargeable aluminum batteries. *Prog Mater Sci* 2022;128:100960. DOI

37.   Yu X, Manthiram A. Electrochemical energy storage with a reversible nonaqueous room-temperature aluminum-sulfur chemistry. *Adv Energy Mater* 2017;7:1700561. DOI

38.   Buckingham R, Asset T, Atanassov P. Aluminum-air batteries: a review of alloys, electrolytes and design. *J Power Sources* 2021;498:229762. DOI

39.   Tu J, Wang S, Li S, Wang C, Sun D, Jiao S. The effects of anions behaviors on electrochemical properties of Al/graphite rechargeable aluminum-ion battery via molten $AlCl_3$-NaCl liquid electrolyte. *J Electrochem Soc* 2017;164:A3292-302. DOI

40.   Elia GA, Hasa I, Greco G, et al. Insights into the reversibility of aluminum graphite batteries. *J Mater Chem A* 2017;5:9682-90. DOI

41.   Kravchyk KV, Wang S, Piveteau L, Kovalenko MV. Efficient aluminum chloride-natural graphite battery. *Chem Mater* 2017;29:4484-92. DOI

42. Abood HM, Abbott AP, Ballantyne AD, Ryder KS. Do all ionic liquids need organic cations? Characterisation of $[AlCl_2 \cdot nAmide]^+$ $AlCl_4^-$ and comparison with imidazolium based systems. *Chem Commun* ;47:3523-5. DOI

43. Fang Y, Jiang X, Sun XG, Dai S. New ionic liquids based on the complexation of dipropyl sulfide and $AlCl_3$ for electrodeposition of aluminum. *Chem Commun* 2015;51:13286-9. DOI PubMed

44. Hu P, Zhang R, Meng X, Liu H, Xu C, Liu Z. Structural and spectroscopic characterizations of amide-$AlCl_3$-based ionic liquid analogues. *Inorg Chem* 2016;55:2374-80. DOI

45. Xu H, Bai T, Chen H, et al. Low-cost $AlCl_3/Et_3NHCl$ electrolyte for high-performance aluminum-ion battery. *Energy Stor Mater* 2019;17:38-45. DOI

46. Liu Z, Wang X, Liu Z, et al. Low-cost gel polymer electrolyte for high-performance aluminum-ion batteries. *ACS Appl Mater Interfaces* 2021;13:28164-70. DOI

47. Sun XG, Fang Y, Jiang X, Yoshii K, Tsuda T, Dai S. Polymer gel electrolytes for application in aluminum deposition and rechargeable aluminum ion batteries. *Chem Commun* 2016;52:292-5. DOI PubMed

48. Yu Z, Jiao S, Tu J, et al. Gel electrolytes with a wide potential window for high-rate Al-ion batteries. *J Mater Chem A* 2019;7:20348-56. DOI

49. Wu F, Yang H, Bai Y, Wu C. Paving the path toward reliable cathode materials for aluminum-ion batteries. *Adv Mater* 2019;31:e1806510. DOI

50. Zhu N, Wu F, Wang Z, et al. Reversible Al^{3+} storage mechanism in anatase TiO_2 cathode material for ionic liquid electrolyte-based aluminum-ion batteries. *J Energy Chem* 2020;51:72-80. DOI

51. Zhang L, Chen L, Luo H, Zhou X, Liu Z. Large-sized few-layer graphene enables an ultrafast and long-life aluminum-ion battery. *Adv Energy Mater* 2017;7:1700034. DOI

52. Wu Y, Gong M, Lin MC, et al. 3D graphitic foams derived from chloroaluminate anion intercalation for ultrafast aluminum-ion battery. *Adv Mater* 2016;28:9218-22. DOI

53. Geng L, Scheifers JP, Fu C, Zhang J, Fokwa BPT, Guo J. Titanium sulfides as intercalation-type cathode materials for rechargeable aluminum batteries. *ACS Appl Mater Interfaces* 2017;9:21251-7. DOI

54. Placke T, Fromm O, Lux SF, et al. Reversible intercalation of bis(trifluoromethanesulfonyl)imide anions from an ionic liquid electrolyte into graphite for high performance dual-ion cells. *J Electrochem Soc* 2012;159:A1755-65. DOI

55. Reed LD, Ortiz SN, Xiong M, Menke EJ. A rechargeable aluminum-ion battery utilizing a copper hexacyanoferrate cathode in an organic electrolyte. *Chem Commun* 2015;51:14397-400. DOI

56. Wang S, Yu Z, Tu J, et al. A novel aluminum-ion battery: $Al/AlCl_3$-[EMIm]Cl/Ni_3S_2@Graphene. *Adv Energy Mater* 2016;6:1600137. DOI

57. Wang S, Jiao S, Wang J, et al. High-performance aluminum-ion battery with CuS@C microsphere composite cathode. *ACS Nano* 2017;11:469-77. DOI

58. Zhang C, Mahmood N, Yin H, Liu F, Hou Y. Synthesis of phosphorus-doped graphene and its multifunctional applications for oxygen reduction reaction and lithium ion batteries. *Adv Mater* 2013;25:4932-7. DOI PubMed

59. Yousaf M, Naseer U, Li Y, et al. A mechanistic study of electrode materials for rechargeable batteries beyond lithium ions by *in situ* transmission electron microscopy. *Energy Environ Sci* 2021;14:2670-707. DOI

60. Mahmood N, Zhang C, Yin H, Hou Y. Graphene-based nanocomposites for energy storage and conversion in lithium batteries, supercapacitors and fuel cells. *J Mater Chem A* 2014;2:15-32. DOI

61. Tareen AK, Khan K, Iqbal M, et al. Recent advance in two-dimensional MXenes: new horizons in flexible batteries and supercapacitors technologies. *Energy Stor Mater* 2022;53:783-826. DOI

62. Tahir M, Cao C, Butt FK, et al. Tubular graphitic-C_3N_4: a prospective material for energy storage and green photocatalysis. *J Mater Chem A* 2013;1:13949. DOI

63. Goel P, Dobhal D, Sharma R. Aluminum-air batteries: a viability review. *J Energy Stor* 2020;28:101287. DOI

64. Mori R. Recent developments for aluminum-air batteries. *Electrochem Energy Rev* 2020;3:344-69. DOI

65. Gaele MF, Di Palma TM. Rechargeable aluminum-air batteries based on aqueous solid-state electrolytes. *Energy Technol* 2022;10:2101046. DOI

66. Fan L, Lu H. The effect of grain size on aluminum anodes for Al-air batteries in alkaline electrolytes. *J Power Sources* 2015;284:409-15. DOI

67. Fan L, Lu H, Leng J, Sun Z, Chen C. The effect of crystal orientation on the aluminum anodes of the aluminum-air batteries in alkaline electrolytes. *J Power Sources* 2015;299:66-9. DOI

68. Wu Z, Zhang H, Qin K, et al. The role of gallium and indium in improving the electrochemical characteristics of Al-Mg-Sn-based alloy for Al-air battery anodes in 2 M NaCl solution. *J Mater Sci* 2020;55:11545-60. DOI

69. Zhuang Z, Feng Y, Peng C, Yang L, Wang M. Effect of Ga on microstructure and electrochemical performance of Al-0.4Mg-0.05Sn-0.03Hg alloy as anode for Al-air batteries. *Trans Nonferr Metal Soc* 2021;31:2558-69. DOI

70. Ren J, Fu C, Dong Q, et al. Evaluation of impurities in aluminum anodes for Al-air batteries. *ACS Sustain Chem Eng* 2021;9:2300-8. DOI

71. Lv C, Li Y, Zhu Y, et al. Quasi-solid-state aluminum-air batteries with ultra-high energy density and uniform aluminum stripping behavior. *Adv Sci* 2023;10:e2304214. DOI PubMed PMC

72. Wang Y, Pan W, Leong KW, Luo S, Zhao X, Leung DY. Solid-state Al-air battery with an ethanol gel electrolyte. *Green Energy*

Environ 2023;8:1117-27. DOI

73.   Harchegani RK, Riahi AR. Synergistic effect of vanadate and nanoclay hybrid inhibitor on the self-corrosion and discharge activity of Al anode in alkaline aluminum-air batteries. *J Electrochem Soc* 2023;170:030524. DOI

74.   Srivastava S, Ahuja D, Varshney PK. Impact of surface modification of electrode for aluminium air batteries. *J Energy Stor* 2024;76:109588. DOI

75.   Zuo Y, Yu Y, Liu H, Gu Z, Cao Q, Zuo C. Electrospun Al_2O_3 film as inhibiting corrosion interlayer of anode for solid aluminum-air batteries. *Batteries* 2020;6:19. DOI

76.   Zuo Y, Yu Y, Shi H, Wang J, Zuo C, Dong X. Inhibition of hydrogen evolution by a bifunctional membrane between anode and electrolyte of aluminum-air battery. *Membranes* 2022;12:407. DOI PubMed PMC

77.   Ipadeola AK, Eid K, Abdullah AM. Porous transition metal-based nanostructures as efficient cathodes for aluminium-air batteries. *Curr Opin Electrochem* 2023;37:101198. DOI

78.   Timofeeva EV, Segre CU, Pour GS, Vazquez M, Patawah BL. Aqueous air cathodes and catalysts for metal-air batteries. *Curr Opin Electrochem* 2023;38:101246. DOI

79.   Meng X, Zhang X, Rageloa J, Liu Z, Wang W. Coordination strategy to prepare high-performance Fe-Nx catalysts for Al-air batteries. *J Power Sources* 2023;567:232988. DOI

80.   Yu Y, Zuo Y, Liu Y, et al. Directly electrospun carbon nanofibers incorporated with Mn_3O_4 nanoparticles as bending-resistant cathode for flexible Al-air batteries. *Nanomaterials* 2020;10:216. DOI PubMed PMC

81.   Ma Y, Sumboja A, Zang W, et al. Flexible and wearable all-solid-state Al-air battery based on iron carbide encapsulated in electrospun porous carbon nanofibers. *ACS Appl Mater Interfaces* 2019;11:1988-95. DOI

82.   Li K, Wang C, Li H, et al. Heterostructural interface in Fe_3C-TiN quantum dots boosts oxygen reduction reaction for Al-air batteries. *ACS Appl Mater Interfaces* 2021;13:47440-8. DOI

83.   Liu D, Tian J, Tang Y, et al. High-power double-face flow Al-air battery enabled by CeO_2 decorated MnOOH nanorods catalyst. *Chem Eng J* 2021;406:126772. DOI

84.   Akgenc B, Sarikurt S, Yagmurcukardes M, Ersan F. Aluminum and lithium sulfur batteries: a review of recent progress and future directions. *J Phys Condens Matter* 2021;33:253002. DOI PubMed

85.   Cheng R, Jiang M, Li K, et al. Dimensional engineering of carbon dots derived sulfur and nitrogen co-doped carbon as efficient oxygen reduction reaction electrocatalysts for aluminum-air batteries. *Chem Eng J* 2021;425:130603. DOI

86.   Wang M, Li Y, Fang J, et al. Superior oxygen reduction reaction on phosphorus-doped carbon dot/graphene aerogel for all-solid-state flexible Al-air batteries. *Adv Energy Mater* 2020;10:1902736. DOI

87.   Shui Z, Liao X, Lei Y, et al. MnO_2 synergized with N/S codoped graphene as a flexible cathode efficient electrocatalyst for advanced honeycomb-shaped stretchable aluminum-air batteries. *Langmuir* 2020;36:12954-62. DOI

88.   Wang Z, Zhou H, Xue J, et al. Ultrasonic-assisted hydrothermal synthesis of cobalt oxide/nitrogen-doped graphene oxide hybrid as oxygen reduction reaction catalyst for Al-air battery. *Ultrason Sonochem* 2021;72:105457. DOI PubMed PMC

89.   Huang L, Zang W, Ma Y, et al. In-situ formation of isolated iron sites coordinated on nitrogen-doped carbon coated carbon cloth as self-supporting electrode for flexible aluminum-air battery. *Chem Eng J* 2021;421:129973. DOI

90.   Long G, Liu Y, Chen M, et al. Effects of ultrasound on synthesis and performance of manganese-based/ graphene oxide oxygen reduction catalysts for aluminum-air batteries. *J Power Sources* 2023;573:233150. DOI

91.   Xia Z, Zhu Y, Zhang W, et al. Cobalt ion intercalated MnO_2/C as air cathode catalyst for rechargeable aluminum-air battery. *J Alloys Compd* 2020;824:153950. DOI

92.   Hosseini S, Chiu C, Pourzolfaghar H, Su C, Li Y. Techno-economically feasible beverage can as superior anode in rechargeable Al-air batteries. *Sustain Mater Technol* 2023;35:e00560. DOI

93.   Yu L, Xu N, Zhu T, Xu Z, Sun M, Geng D. $La_{0.4}Sr_{0.6}Co_{0.7}Fe_{0.2}Nb_{0.1}O_{3-\delta}$ perovskite prepared by the sol-gel method with superior performance as a bifunctional oxygen electrocatalyst. *Int J Hydrogen Energy* 2020;45:30583-91. DOI

94.   Shui Z, Zhao W, Xiao H, et al. Controllable porous perovskite with three-dimensional ordered structure as an efficient oxygen reduction reaction electrocatalyst for flexible aluminum-air battery. *J Power Sources* 2022;523:231028. DOI

95.   Chen J, Zhu Q, Jiang L, et al. Rechargeable aqueous aluminum organic batteries. *Angew Chem Int Ed* 2021;60:5794-9. DOI

96.   Yoo D, Kim J, Shin J, Kim KJ, Choi JW. Stable performance of aluminum-metal battery by incorporating lithium-ion chemistry. *ChemElectroChem* 2017;4:2345-51. DOI

97.   Sun XG, Zhang Z, Guan H, et al. A sodium-aluminum hybrid battery. *Meet Abstr* 2017;MA2017-02:564. DOI

98.   Ramasubramanian B, Sundarrajan S, Chellappan V, Reddy MV, Ramakrishna S, Zaghib K. Recent development in carbon-LiFePO₄ cathodes for lithium-ion batteries: a mini review. *Batteries* 2022;8:133. DOI

99.   Zeng X, Peng J, Guo Y, Zhu H, Huang X. Research progress on $Na_3V_2(PO_4)_3$ cathode material of sodium ion battery. *Front Chem* 2020;8:635. DOI PubMed PMC

100. Ji B, Zhang F, Sheng M, Tong X, Tang Y. A Novel and generalized lithium-ion-battery configuration utilizing Al foil as both anode and current collector for enhanced energy density. *Adv Mater* 2017;29:1604219. DOI

101. Parans Paranthaman M, Liu H, Sun XG, Dai S, Brown GM. Chapter 13 - aluminum-ion batteries for medium- and large-scale energy storage. In: Advances in batteries for medium and large-scale energy storage. Elsevier; 2015. pp. 463-74. DOI

102. Ghavidel MZ, Kupsta MR, Le J, Feygin E, Espitia A, Fleischauer MD. Electrochemical formation of four Al-Li phases (β-AlLi, Al_2Li_3, $AlLi_{2-x}$, Al_4Li_9) at intermediate temperatures. *J Electrochem Soc* 2019;166:A4034-40. DOI

103. Li D, Chu F, He Z, Cheng Y, Wu F. Single-material aluminum foil as anodes enabling high-performance lithium-ion batteries: the roles of prelithiation and working mechanism. *Mater Today* 2022;58:80-90. DOI

104. Wang H, Tan H, Luo X, et al. The progress on aluminum-based anode materials for lithium-ion batteries. *J Mater Chem A* 2020;8:25649-62. DOI

105. Zheng T, Boles ST. Lithium aluminum alloy anodes in Li-ion rechargeable batteries: past developments, recent progress, and future prospects. *Prog Energy* 2023;5:032001. DOI

106. Li H, Yamaguchi T, Matsumoto S, et al. Circumventing huge volume strain in alloy anodes of lithium batteries. *Nat Commun* 2020;11:1584. DOI PubMed PMC

107. Zhang W. A review of the electrochemical performance of alloy anodes for lithium-ion batteries. *J Power Sources* 2011;196:13-24. DOI

108. Gu X, Dong J, Lai C. Li-containing alloys beneficial for stabilizing lithium anode: a review. *Eng Rep* 2021;3:e12339. DOI

109. Sun J, Zeng Q, Lv R, et al. A Li-ion sulfur full cell with ambient resistant Al-Li alloy anode. *Energy Stor Mater* 2018;15:209-17. DOI

110. Ryu J, Kang J, Kim H, Lee JH, Lee H, Park S. Electrolyte-mediated nanograin intermetallic formation enables superionic conduction and electrode stability in rechargeable batteries. *Energy Stor Mater* 2020;33:164-72. DOI

111. Zheng T, Kramer D, Mönig R, Boles ST. Aluminum foil anodes for Li-ion rechargeable batteries: the role of Li solubility within β-LiAl. *ACS Sustain Chem Eng* 2022;10:3203-10. DOI

112. Yu Y, Li S, Fan H, et al. Optimal annealing of Al foil anode for prelithiation and full-cell cycling in Li-ion battery: the role of grain boundaries in lithiation/delithiation ductility. *Nano Energy* 2020;67:104274. DOI

113. Crowley PJ, Scanlan KP, Manthiram A. Diffusional lithium trapping as a failure mechanism of aluminum foil anodes in lithium-ion batteries. *J Power Sources* 2022;546:231973. DOI

114. Chang X, Xie Z, Liu Z, Zheng X, Zheng J, Li X. Enabling high performance lithium storage in aluminum: the double edged surface oxide. *Nano Energy* 2017;41:731-7. DOI

115. Sun X, Yang C, Zhao Y, et al. Ultrathin aluminum nanosheets grown on carbon nanotubes for high performance lithium ion batteries. *Adv Funct Mater* 2022;32:2109112. DOI

116. Gu J, Li B, Du Z, Zhang C, Zhang D, Yang S. Multi-atomic layers of metallic aluminum for ultralong life lithium storage with high volumetric capacity. *Adv Funct Mater* 2017;27:1700840. DOI

117. Zhang M, Xiang L, Galluzzi M, et al. Uniform distribution of alloying/dealloying stress for high structural stability of an Al anode in high-areal-density lithium-ion batteries. *Adv Mater* 2019;31:e1900826. DOI

118. Fan H, Chen B, Li S, et al. Nanocrystalline Li-Al-Mn-Si foil as reversible Li host: electronic percolation and electrochemical cycling stability. *Nano Lett* 2020;20:896-904. DOI

119. Kwon GD, Moyen E, Lee YJ, Joe J, Pribat D. Graphene-coated aluminum thin film anodes for lithium-ion batteries. *ACS Appl Mater Interfaces* 2018;10:29486-95. DOI PubMed

120. Muñoz-torrero D, Leung P, García-quismondo E, et al. Investigation of different anode materials for aluminium rechargeable batteries. *J Power Sources* 2018;374:77-83. DOI

121. Wang P, Chen H, Li N, et al. Dense graphene papers: toward stable and recoverable Al-ion battery cathodes with high volumetric and areal energy and power density. *Energy Stor Mater* 2018;13:103-11. DOI

122. Yan C, Lv C, Wang L, et al. Architecting a stable high-energy aqueous Al-ion battery. *J Am Chem Soc* 2020;142:15295-304. DOI

123. Sovizi M, Afshari M. Effect of nano zirconia on electrochemical performance, corrosion behavior and microstructure of Al-Mg-Sn-Ga anode for aluminum batteries. *J Alloys Compd* 2019;792:1088-94. DOI

124. Asfia MP, Pourfarzad H, Kashani H, Olia MH, Badrnezhad R. Study of uniform and localized corrosion behaviour of aluminum alloy 1050 as Al/AgO battery anode in aerated NaCl in the presence of an organosulfur inhibitor. *J Electrochem Soc* 2020;167:140527. DOI

125. Chen H, Xu H, Zheng B, et al. Oxide film efficiently suppresses dendrite growth in aluminum-ion battery. *ACS Appl Mater Interfaces* 2017;9:22628-34. DOI

126. Ran Q, Shi H, Meng H, et al. Aluminum-copper alloy anode materials for high-energy aqueous aluminum batteries. *Nat Commun* 2022;13:576. DOI PubMed PMC

127. Zheng J, Bock DC, Tang T, et al. Regulating electrodeposition morphology in high-capacity aluminium and zinc battery anodes using interfacial metal-substrate bonding. *Nat Energy* 2021;6:398-406. DOI

128. Shen X, Sun T, Yang L, et al. Ultra-fast charging in aluminum-ion batteries: electric double layers on active anode. *Nat Commun* 2021;12:820. DOI PubMed PMC

129. Afshari M, Abbasi R, Sovizi MR. Evaluation of nanometer-sized zirconium oxide incorporated Al-Mg-Ga-Sn alloy as anode for alkaline aluminum batteries. *Trans Nonferr Metal Soc* 2020;30:90-8. DOI

130. Mahmood N, De Castro IA, Pramoda K, Khoshmanesh K, Bhargava SK, Kalantar-zadeh K. Atomically thin two-dimensional metal oxide nanosheets and their heterostructures for energy storage. *Energy Stor Mater* 2019;16:455-80. DOI

131. Mahmood N, Hou Y. Electrode nanostructures in lithium-based batteries. *Adv Sci* 2014;1:1400012. DOI PubMed PMC

132. Kuksenko SP. Aluminum foil as anode material of lithium-ion batteries: effect of electrolyte compositions on cycling parameters. *Russ J Electrochem* 2013;49:67-75. DOI

133. Hamon Y, Brousse T, Jousse F, Topart P, Buvat P, Schleich D. Aluminum negative electrode in lithium ion batteries. *J Power*

Sources 2001;97-98:185-7.   DOI

134.   Du W, Ang EH, Yang Y, Zhang Y, Ye M, Li CC. Challenges in the material and structural design of zinc anode towards high-performance aqueous zinc-ion batteries. *Energy Environ Sci* 2020;13:3330-60.   DOI

135.   Li Z, Liu J, Niu B, Li J, Kang F. A Novel graphite-graphite dual ion battery using an $AlCl_3$-[EMIm]Cl liquid electrolyte. *Small* 2018;14:e1800745.   DOI

136.   Song Y, Jiao S, Tu J, et al. A long-life rechargeable Al ion battery based on molten salts. *J Mater Chem A* 2017;5:1282-91.   DOI

137.   Wedepohl K. The composition of the continental crust. *Geochim Cosmochim Acta* 1995;59:1217-32.   DOI

138.   Tang W, Zhu Y, Hou Y, et al. Aqueous rechargeable lithium batteries as an energy storage system of superfast charging. *Energy Environ Sci* 2013;6:2093.   DOI

139.   Wang D, Zeng Q, Zhou G, et al. Carbon-sulfur composites for Li-S batteries: status and prospects. *J Mater Chem A* 2013;1:9382.   DOI

140.   Li X, Wei B. Supercapacitors based on nanostructured carbon. *Nano Energy* 2013;2:159-73.   DOI

141.   Xu C, Xu B, Gu Y, Xiong Z, Sun J, Zhao XS. Graphene-based electrodes for electrochemical energy storage. *Energy Environ Sci* 2013;6:1388.   DOI

142.   Rani JV, Kanakaiah V, Dadmal T, Rao MS, Bhavanarushi S. Fluorinated natural graphite cathode for rechargeable ionic liquid based aluminum-ion battery. *J Electrochem Soc* 2013;160:A1781-4.   DOI

143.   Levitin G, Yarnitzky C, Licht S. Fluorinated graphites as energetic cathodes for nonaqueous Al batteries. *Electrochem Solid State Lett* 2002;5:A160.   DOI

144.   Li Z, Huang Y, Yuan L, Hao Z, Huang Y. Status and prospects in sulfur-carbon composites as cathode materials for rechargeable lithium-sulfur batteries. *Carbon* 2015;92:41-63.   DOI

145.   Zhang K, Kirlikovali KO, Varma RS, et al. Covalent organic frameworks: emerging organic solid materials for energy and electrochemical applications. *ACS Appl Mater Interfaces* 2020;12:27821-52.   DOI

146.   Tu J, Wang J, Li S, et al. High-efficiency transformation of amorphous carbon into graphite nanoflakes for stable aluminum-ion battery cathodes. *Nanoscale* 2019;11:12537-46.   DOI

147.   Wang S, Kravchyk KV, Krumeich F, Kovalenko MV. Kish graphite flakes as a cathode material for an aluminum chloride-graphite battery. *ACS Appl Mater Interfaces* 2017;9:28478-85.   DOI PubMed

148.   Ellingsen LA, Holland A, Drillet JF, et al. Environmental screening of electrode materials for a rechargeable aluminum battery with an $AlCl_3$/EMIMCl electrolyte. *Materials* 2018;11:936.   DOI PubMed PMC

149.   Murphy DW, Christian PA, Disalvo FJ, Carides JN, Waszczak JV. Lithium Incorporation by V_6O_{13} and related vanadium (+4, +5) oxide cathode materials. *J Electrochem Soc* 1981;128:2053-60.   DOI

150.   Zhang C, He R, Zhang J, Hu Y, Wang Z, Jin X. Amorphous carbon-derived nanosheet-bricked porous graphite as high-performance cathode for aluminum-ion batteries. *ACS Appl Mater Interfaces* 2018;10:26510-6.   DOI

151.   Yan Q, Shen Y, Miao Y, Wang M, Yang M, Zhao X. Vanadium oxychloride as cathode for rechargeable aluminum batteries. *J Alloys Compd* 2019;806:1109-15.   DOI

152.   Shi M, Wei W, Jiang Z, Han H, Gao J, Xie J. Biomass-derived multifunctional TiO_2/carbonaceous aerogel composite as a highly efficient photocatalyst. *RSC Adv* 2016;6:25255-66.   DOI

153.   Hu Z, Zhang H, Wang H, Zhang F, Li Q, Li H. Nonaqueous aluminum ion batteries: recent progress and prospects. *ACS Mater Lett* 2020;2:887-904.   DOI

154.   González JR, Nacimiento F, Cabello M, Alcántara R, Lavela P, Tirado JL. Reversible intercalation of aluminium into vanadium pentoxide xerogel for aqueous rechargeable batteries. *RSC Adv* 2016;6:62157-64.   DOI

155.   Hong H, Liu J, Huang H, et al. Ordered macro-microporous metal-organic framework single crystals and their derivatives for rechargeable aluminum-ion batteries. *J Am Chem Soc* 2019;141:14764-71.   DOI

156.   Hu Y, Huang H, Yu D, et al. All-climate aluminum-ion batteries based on binder-free MOF-derived FeS_2@C/CNT cathode. *Nanomicro Lett* 2021;13:159.   DOI PubMed PMC

157.   Gu S, Wang H, Wu C, Bai Y, Li H, Wu F. Confirming reversible Al^{3+} storage mechanism through intercalation of Al^{3+} into V_2O_5 nanowires in a rechargeable aluminum battery. *Energy Stor Mater* 2017;6:9-17.   DOI

158.   Nethravathi C, Viswanath B, Michael J, Rajamath M. Hydrothermal synthesis of a monoclinic VO_2 nanotube-graphene hybrid for use as cathode material in lithium ion batteries. *Carbon* 2012;50:4839-46.   DOI

159.   Jiang J, Feng Y, Mahmood N, Liu F, Hou Y. SnS_2/graphene composites: excellent anode materials for lithium ion battery and photolysis catalysts. *Sci Adv Mat* 2013;5:1667-75.   DOI

160.   Choi S, Go H, Lee G, Tak Y. Electrochemical properties of an aluminum anode in an ionic liquid electrolyte for rechargeable aluminum-ion batteries. *Phys Chem Chem Phys* 2017;19:8653-6.   DOI

161.   Jiao H, Wang C, Tu J, Tian D, Jiao S. A rechargeable Al-ion battery: Al/molten $AlCl_3$-urea/graphite. *Chem Commun* 2017;53:2331-4.   DOI

162.   Wang C, Li J, Jiao H, Tu J, Jiao S. The electrochemical behavior of an aluminum alloy anode for rechargeable Al-ion batteries using an $AlCl_3$-urea liquid electrolyte. *RSC Adv* 2017;7:32288-93.   DOI

163.   Zhu N, Zhang K, Wu F, Bai Y, Wu C. Ionic liquid-based electrolytes for aluminum/magnesium/sodium-ion batteries. *Energy Mater Adv* 2021;2021:9204217.   DOI

164.   Rehman S, Gu X, Khan K, et al. 3D vertically aligned and interconnected porous carbon nanosheets as sulfur immobilizers for high

performance lithium-sulfur batteries. *Adv Energy Mat J* 2016;6:1502518. DOI

165.   Huang X, Liu Y, Liu C, Zhang J, Noonan O, Yu C. Rechargeable aluminum-selenium batteries with high capacity. *Chem Sci* 2018;9:5178-82. DOI PubMed PMC

166.   Hu Y, Sun D, Luo B, Wang L. Recent progress and future trends of aluminum batteries. *Energy Technol* 2019;7:86-106. DOI

167.   Nasim Khan RN, Mahmood N, Lv C, et al. Pristine organo-imido polyoxometalates as an anode for lithium ion batteries. *RSC Adv* 2014;4:7374. DOI

168.   Lin MC, Gong M, Lu B, et al. An ultrafast rechargeable aluminium-ion battery. *Nature* 2015;520:325-8. DOI

169.   Kim I, Jang S, Lee KH, Tak Y, Lee G. In situ polymerized solid electrolytes for superior safety and stability of flexible solid-state Al-ion batteries. *Energy Stor Mater* 2021;40:229-38. DOI

170.   Lee D, Lee G, Tak Y. Hypostatic instability of aluminum anode in acidic ionic liquid for aluminum-ion battery. *Nanotechnology* 2018;29:36LT01. DOI

171.   Wu F, Zhu N, Bai Y, Gao Y, Wu C. An interface-reconstruction effect for rechargeable aluminum battery in ionic liquid electrolyte to enhance cycling performances. *Green Energy Environ* 2018;3:71-7. DOI

172.   Wang H, Gu S, Bai Y, et al. Anion-effects on electrochemical properties of ionic liquid electrolytes for rechargeable aluminum batteries. *J Mater Chem A* 2015;3:22677-86. DOI